General Disclaimer

One or more of the Following Statements may affect this Document

- This document has been reproduced from the best copy furnished by the organizational source. It is being released in the interest of making available as much information as possible.

- This document may contain data, which exceeds the sheet parameters. It was furnished in this condition by the organizational source and is the best copy available.

- This document may contain tone-on-tone or color graphs, charts and/or pictures, which have been reproduced in black and white.

- This document is paginated as submitted by the original source.

- Portions of this document are not fully legible due to the historical nature of some of the material. However, it is the best reproduction available from the original submission.

JPL PUBLICATION 79-99

Homogeneous Vortex Model for Liquid Slosh in Spinning Spherical Tanks

Michael El-Raheb
Paul Wagner

November 15, 1979

National Aeronautics and
Space Administration

Jet Propulsion Laboratory
California Institute of Technology
Pasadena, California

TECHNICAL REPORT STANDARD TITLE PAGE

1. Report No. JPL PUB. 79-99	2. Government Accession No.	3. Recipient's Catalog No.
4. Title and Subtitle Homogeneous Vortex Model for Liquid Slosh in Spinning Spherical Tanks		5. Report Date November 15, 1979 6. Performing Organization Code
7. Author(s) Michael El-Raheb and Paul Wagner		8. Performing Organization Report No.
9. Performing Organization Name and Address JET PROPULSION LABORATORY California Institute of Technology 4800 Oak Grove Drive Pasadena, California 91103		10. Work Unit No. 11. Contract or Grant No. NAS 7-100 13. Type of Report and Period Covered JPL Publication
12. Sponsoring Agency Name and Address NATIONAL AERONAUTICS AND SPACE ADMINISTRATION Washington, D.C. 20546		14. Sponsoring Agency Code

15. Supplementary Notes

16. Abstract

The problem of forced fluid sloshing in a partially filled spinning spherical tank is solved numerically using the finite element method. The governing equations include Coriolis acceleration, empirical fluid damping and spatially homogeneous vorticity first introduced by Pfeiffer. An exponential instability similar to flutter is detected in the present simulation for fill ratios below 50%. This instability appears in the model as a result of the homogeneous vortex assumption since the free slosh equations are neutrally stable in the Liapunov sense.

17. Key Words (Selected by Author(s))	18. Distribution Statement
Astronautics (General) Fluid Mechanics and Heat Transfer Fluid Mechanics Solid Propellants	Unclassified - Unlimited

19. Security Classif. (of this report)	20. Security Classif. (of this page)	21. No. of Pages	22. Price
Unclassified	Unclassified	48	

JPL PUBLICATION 79-99

Homogeneous Vortex Model for Liquid Slosh in Spinning Spherical Tanks

Michael El-Raheb
Paul Wagner

November 15, 1979

National Aeronautics and
Space Administration

Jet Propulsion Laboratory
California Institute of Technology
Pasadena, California

The research described in this publication was carried out by the Jet Propulsion Laboratory, California Institute of Technology, under NASA Contract No. NAS7-100.

ACKNOWLEDGEMENT

The major portion of this work was performed for and was sponsored by the Galileo Flight Project. The effort was partially supported by A. Amos and R. Goetz, Office of Aeronautics and Space Technology at NASA.

We wish to express our appreciation to Professor T. K. Caughey of the Applied Mechanics Department, California Institute of Technology, for his constructive suggestions regarding the stability analysis and his help in assessing the initial slosh analysis.

Appreciation is also extended to Dr. A. Pohl of Messerschmitt-Bölkow-Blohm in Munich for his preliminary work.

ABSTRACT

The problem of forced fluid sloshing in a partially filled spinning spherical tank is solved numerically using the finite element method. The governing equations include Coriolis acceleration, empirical fluid damping and spatially homogeneous vorticity first introduced by Pfeiffer. An exponential instability similar to flutter is detected in the present simulation for fill ratios below 50%. This instability appears in the model as a result of the homogeneous vortex assumption since the free slosh equations are neutrally stable in the Liapunov sense.

CONTENTS

I. SUMMARY 1

II. INTRODUCTION 2

III. EQUATIONS OF MOTION 3

IV. SLOSH FORCES AND MOMENTS 14

V. PROCESS OF SOLUTION 17

VI. SLOSH DAMPING SIMULATION 19

VII. NUMERICAL RESULTS 22

VIII. STABILITY ANALYSIS OF FREE SLOSHING 24

REFERENCES 27

Figures

1. Reference and local rotating coordinate systems 28

2. Accelerations on fluid volume 28

3. Comparison for translational slosh 29

4. Nondimensional tangential slosh force for case A 29

5. Nondimensional tangential slosh force for case B 30

6. Nondimensional tangential slosh force for case C 30

7. Stability boundary 31

8a. Characteristic frequencies for $\tilde{V} = 0.03$ 32

8b. Characteristic damping for $\tilde{V} = 0.03$ 32

9a. Characteristic frequencies for $\tilde{V} = 0.10$ 33

9b. Characteristic damping for $\tilde{V} = 0.10$ 33

10a. Characteristic frequencies for $\tilde{V} = 0.22$ 34

10b. Characteristic damping for $\tilde{V} = 0.22$ 34

11a. Characteristic frequencies for $\tilde{V} = 0.35$ 35

Figures

11b. Characteristic damping for $\tilde{V} = 0.35$ 35

12a. Characteristic frequencies for $\tilde{V} = 0.43$ 36

12b. Characteristic damping for $\tilde{V} = 0.43$ 36

13a. Characteristic frequencies for $\tilde{V} = 0.50$ 37

13b. Characteristic damping for $\tilde{V} = 0.50$ 37

14a. Characteristic frequencies for $\tilde{V} = 0.57$ 38

14b. Characteristic damping for $\tilde{V} = 0.57$ 38

15. Variation of nondimensional negative damping with β . . . 39

Table

1. Representative test cases 23

I. SUMMARY

The Galileo dual-spin Jupiter orbiter spacecraft carries an amount of fluid that represents about half of the total weight. The fluid is contained in four tanks symmetrically located about the spin axis of the spacecraft. In order to evaluate the behavior of the fluid slosh in the spinning configuration as it affects the attitude control, an analysis was initiated early in the project. An analytical slosh model that accounts for the steady spacecraft spin was performed by Messerschmitt-Bölkow-Blohm Company (MBB), at Munich, W. Germany, as part of the effort of manufacturing the retro-propulsion module for the Galileo spacecraft. The MBB analysis had several simplifying assumptions:

(a) In order to arrive at a practically solvable set of equations, the vorticity was taken to be independent of the spatial coordinates while it is a function of time only. This model was first introduced by Pfeiffer at MBB in 1974.

(b) The steady-state spin as well as angular perturbation was felt instantaneously in the fluid. This assumption is inconsistent with the mechanism of vortex transfer from the tank wall into the fluid.

(c) The Coriolis acceleration was retained inside the fluid but was neglected in the free surface pressure boundary conditions in order to arrive at an exact differential form.

The assumption of homogeneous vorticity was found to lead to fictitious instabilities for certain fluid fill ratios. The inconsistency of this model was further substantiated by a stability analysis performed by T. K. Caughey, who showed that a Liapunov function of the free vibration equations had a vanishing first time derivative leading to a neutrally stable system. It was concluded that the MBB analysis is only valid for fluid fills above 55%.

An equivalent simplified dynamic pendulum model to represent the fuel slosh was proposed for quick assessment of the fluid effect on the attitude control system. Further investigation by JPL concluded that it is impossible to achieve such a simplified equivalence for rotating tanks where Coriolis acceleration and vorticity prevail. Therefore, a pendulum model can only give an incomplete fluid behavior representation.

A complete analytical investigation of the fluid behavior is now believed to be a very complex undertaking that for cost and schedule reasons is not recommended. Instead, a testing program of the complete spacecraft with its appropriate inertia, fluid fill, and spin rates is suggested to obtain an understanding of the attitude control/fluid interaction.

II. INTRODUCTION

The problem of liquid slosh in spinning containers has lately received substantial attention as it is an essential step in analytically assessing the destabilizing energy dissipation in dual-spin spacecraft. The solution of the governing equations is involved due to the occurrence of the Coriolis term which destroys the self-adjointness of the Euler equations. An alternate set of equations that excludes the pressure gradient can be obtained by applying the curl operator on the Euler equations, thus obtaining the Helmholtz equation of vorticity.

In 1974, Pfeiffer (Ref. 1) introduced the concept of homogenous vorticity; he argued that the spatially independent vorticity assumes the value of its average over the fluid volume. Although the assumption is valid for completely filled ellipsodial cavities, it is only an approximation for a partially filled cavity.

The fluid perturbation velocity relative to rotating coordinates fixed in the center of the tank is expressed by:

$$\bar{u} = -\nabla\phi - \bar{\Omega} \cdot \bar{\psi} + \bar{\Omega} \times \bar{r}$$

where ϕ is a velocity potential, $\bar{\Omega}$ is the homogenous vortex vector, and $\bar{\psi}$ is the Stokes-Zhukovsky potential. The process of solution starts with the determination of trial functions ϕ_n satisfying the problem:

$$\nabla^2\phi_n = 0 \qquad \text{in } V$$

$$\frac{\partial\phi_n}{\partial n} = \frac{\sigma_n^2}{g}\phi_n \qquad \text{on } S_F \quad \text{(free surface)}$$

$$\frac{\partial\phi_n}{\partial n} = 0 \qquad \text{on } S_W \quad \text{(wetted surface)}$$

where σ_n are the eigenvalues of the potential slosh problem. The potential $\bar{\psi}$ satisfies the problem:

$$\nabla^2\bar{\psi} = 0 \qquad \text{in } V$$

$$\frac{\partial\bar{\psi}}{\partial n} = \bar{r} \times \bar{n} \qquad \text{on } S_F + S_W$$

Substituting the set $\{\phi_n, \sigma_n\}$ and $\bar{\psi}$ into the linearized Helmholz equation and free surface boundary conditions and using the orthogonality of the $\{\phi_n\}$ set, we arrive at a system of linear ordinary differential equations in the dependent variables $\bar{\omega}(t)$ and $\sigma_n(t)$ (the generalized coordinates in the trial function expansion).

The steady spin of the spacecraft is assumed to be felt all over the fluid instantaneously, although the periodic angular motions from control and nutation are only transmitted to a very thin boundary layer of fluid adjacent to the wetted surface of the tank with a radial thickness on the order of $\sqrt{\nu/\omega}$, where ν is the kinematic viscosity and ω the frequency.

The method of finite elements was adopted in determining $\{\phi_n, \sigma_n\}$ as well as the coefficients in the resulting ordinary differential equations. Evaluation of the characteristic eigenvalues indicated that the equations possess an instability for a range of the angle β (angle formed by the resultant gravitational acceleration and the spin axis). The phenomenon is very similar to flutter in the fact that two eigenvalues coalesce in the range of instability. As in the case of flutter where bending and torsion frequencies approach each other, the present motion involves the free surface and vortex motions. The range of instability was found to decrease as the fluid volume ratio (V_{fluid}/V_{tank}) increased, up to a 55% volume ratio, beyond which the motion was stable for all β.

A stability analysis was then performed on the original governing equations. A Liapunov functional was established and shown to have a vanishing first time derivative. This proves that the motion is neutrally stable. It would, therefore, appear that the assumption of homogenous vorticity may be true for filling volumes more than 55%, while for lesser volumes this assumption cannot possibly be true, even approximately.

Great care should then be taken in using Pfeiffer's model in flow problems involving intrinsic resonances.

III. EQUATIONS OF MOTION

Let XYZ be a rotating orthogonal coordinate system with origin at the CG of the spacecraft such that the Z corresponds to the spin axis. Let xyz be a local rotating orthogonal coordinate system with its origin at the center of the spinning spherical tank and parallel to XYZ. The angular velocity vector of XYZ with respect to inertial space is:

$$\bar{\omega}_R = \bar{\Omega}_o + \bar{\omega} \qquad (1)$$

where $\bar{\Omega} = \Omega_0 \bar{k}$ is the steady-state spin about Z, and $\bar{\omega}$ is the perturbation angular velocity vector applied to the spacecraft from control, rigid body, and elastic appendage motions.

Let $\bar{R}$ be the position vector from the spacecraft center of mass C to any point P in the volume V or boundary S of the sphere. Then,

$$\bar{R} = \bar{R}_0 + \bar{r} \tag{2}$$

$\bar{R}_0$ is the radius vector from C to the sphere center o, and $\bar{r}$ is the radius vector from o to any point in V or on S (Figure 1).

The total velocity vector at P(x,y,z) is:

$$\bar{v} = \frac{d\bar{R}}{dt} = \frac{d}{dt}(\bar{R}_0 + \bar{r}) = \bar{v}_0 + \bar{u} + \bar{\Omega}_0 \times \bar{r} \tag{3}$$

where $\bar{v}_0 = d\bar{R}_0/dt$, and $\bar{u}$ is the liquid particle velocity relative to (xyz).

At this point it is necessary to understand the mechanisms of transfer of vorticity from the boundary of the tank to the contained fluid. Assume that the tank is motionless for t < to and that the spin about Z reaches its steady-state value of Ω_0 by accelerating smoothly in order not to incur any ripples on the free surface. Vorticity can only be transmitted to the liquid by stresses tangential to the boundary as those generated by viscosity. It can be shown that vortex motion in a viscous fluid is governed by the diffusion equation. It is evident from the solution that the time it takes to achieve a uniform fluid vortex is of the order:

$$t = O\left(\frac{a^2}{4\nu}\right) \tag{4a}$$

where a is the radius of the sphere, and ν is the kinematic viscosity of the liquid. Furthermore, enforcing a steady periodic excitation to the same vorticity equation shows that only a thin boundary layer of fluid is entrained, having a radial thickness of:

$$\delta_r = O\left(\sqrt{\frac{2\nu}{a}}\right) \tag{4b}$$

The results (4a, b) demonstrate that although a steady-state spin equilibrium may be reached throughout the viscous liquid after some transient time, small periodic rotations will never be transmitted in the core of the liquid and can, therefore, be neglected.

The above argument explains the use of $(\bar{\Omega}_o \times \bar{r})$ rather than $(\bar{\omega}_R \times \bar{r})$ in equation (3), since the latter form is inconsistent with the proper mechanism of vortex transmission discussed above.

The total acceleration vector at P(x,y,z) is:

$$\bar{a} = \frac{d\bar{v}}{dt} = \dot{\bar{\omega}} \times \bar{R}_o + \bar{\Omega}_o \times (\bar{\Omega}_o \times \bar{R}) + \frac{d\bar{u}}{dt} + 2\bar{\Omega}_o \times \bar{u} \qquad (5)$$

The centrifugal acceleration term $\bar{\Omega}_o \times (\bar{\Omega}_o \times \bar{R})$ does not include the perturbation angular velocity $\bar{\omega}$, since this latter motion is not felt by the fluid. Using the definition of the substantial derivative d/dt and the identity:

$$\bar{u} \cdot \nabla\bar{u} = \tfrac{1}{2}\nabla\bar{u}^2 - \bar{u} \times (\nabla \times \bar{u})$$

in the momentum equation, we get:

$$\begin{aligned} &\frac{\partial\bar{u}}{\partial t} + \tfrac{1}{2}\nabla\bar{u}^2 - \bar{u} \times (\nabla \times \bar{u}) + 2\bar{\Omega}_o \times \bar{u} \\ &\quad + \dot{\bar{\omega}} \times \bar{R}_o + \bar{\Omega}_o \times (\bar{\Omega}_o \times \bar{R}) = -\frac{1}{\rho}\nabla p + \bar{f} \end{aligned} \qquad (6)$$

where ρ and p are the fluid density and pressure, respectively, and $\bar{f}$ is the constant body force per unit mass. Superscript $(\dot{})$ denotes the partial derivative with respect to time. For an incompressible liquid, the continuity equation has the form:

$$\nabla \cdot \bar{v} = 0 \implies \nabla \cdot \bar{u} = 0 \qquad (7)$$

We distinguish two sets of kinematic boundary conditions:

A Neuman condition on the wetted surface S_W enforcing no flow through the boundary:

$$\bar{v} \cdot \bar{n} = 0 \implies \bar{u} \cdot \bar{n} = 0 \quad \text{on } S_W \qquad (8a)$$

Let $F(R,t) = 0$ be the equation of the free surface. Then,

$$\frac{dF(\bar{R},t)}{dt} = \frac{\partial F(\bar{R},t)}{\partial t} + \bar{u} \cdot \nabla F(\bar{R},t) = 0 \qquad (8b)$$

In addition to the kinematic relations, the dynamic condition of constant pressure at the free surface S_F is imposed:

$$p(\bar{R},t) = \text{constant} \qquad \text{on } S_F \qquad (8c)$$

In general, the relative velocity vector $\bar{u}$ can be expressed as a combination of an irrotational potential and a rotational term to allow for vorticity:

$$\bar{u} = \nabla\varphi + \bar{\Omega} \times \bar{r} \qquad (9)$$

where

$$\frac{1}{2}\nabla \times \bar{v} = \bar{\Omega}_F = \bar{\Omega}_0 + \bar{\Omega}$$

is the total vorticity. Using the definition in (10) and relation (3):

$$2(\bar{\Omega} + \bar{\Omega}_0) = \nabla \times \bar{v} = \nabla \times \bar{u} + \nabla \times (\bar{\Omega}_0 \times \bar{r})$$

$$\Rightarrow \nabla \times \bar{u} = 2(\bar{\Omega} + \bar{\Omega}_0) - \nabla \times (\bar{\Omega}_0 \times \bar{r}) = 2\bar{\Omega}$$

Therefore,

$$-\bar{u} \times (\nabla \times \bar{u}) = 2\bar{\Omega} \times \bar{u}$$

Substituting (9) in (7) leads to:

$$\nabla^2\varphi = 0 \qquad (10)$$

Substituting (9) in (8a), we arrive at the boundary condition for φ:

$$\nabla\varphi \cdot \bar{n} + (\bar{\Omega} \times \bar{r}) \cdot \bar{n} = 0$$

$$\frac{\partial\varphi}{\partial n} = -(\bar{r} \times \bar{n}) \cdot \bar{\Omega} \qquad \text{on } S_W \tag{11}$$

The form of the boundary condition (11) suggests representing φ in the form

$$\varphi = -\phi - \bar{\Omega} \cdot \bar{\psi} \tag{12}$$

We now introduce the concept of homogenous vortex motion (Ref. 1). Assume that the vorticity $\bar{\Omega}$ is independent of the spatial coordinates and is only a function of time. This assumption is an approximation for the partially filled tank, while it is an exact description for rotating motions of ideal fluids totally filling spheroidal containers (Ref. 2). Based on this assumption, (11) can be rewritten as:

$$\frac{\partial\psi}{\partial n} = -(\bar{r} \times \bar{n}) \cdot \bar{\Omega} = -\frac{\partial\bar{\psi}}{\partial n} \cdot \bar{\Omega} - \frac{\partial\phi}{\partial n} \qquad \text{on } S_W$$

Since the operator on $\bar{\psi}$ and associated boundary condition can be prescribed arbitrarily, let:

$$\begin{aligned} \nabla^2\bar{\psi} &= 0 \text{ in } V; \quad \frac{\partial\bar{\psi}}{\partial n} = \bar{r} \times \bar{n} \qquad \text{on } S_W + S_F \\ \Rightarrow \nabla^2\phi &= 0 \text{ in } V; \quad \frac{\partial\phi}{\partial n} = 0 \qquad \text{on } S_W \end{aligned} \tag{13}$$

The Stokes-Zhukovsky potential vector $\bar{\psi}$ is used to satisfy the inhomogenous boundary condition (11). The scalar potential ϕ satisfies a homogenous Neuman condition on S_W and, as will be shown later, the linearized free surface condition. Substituting (13) in (10) with the assumption that $\bar{\Omega} = \bar{\Omega}(t)$:

$$\bar{u} = -\nabla\phi - \bar{\Omega} \cdot \nabla\bar{\psi} + \bar{\Omega} \times \bar{r} \tag{14}$$

The linearized free surface condition is now derived. At first we define the steady-state equilibrium free surface equation by estimating all time-dependent quantities in the momentum equation (6):

$$\bar{\Omega}_o \times (\bar{\Omega}_o \times \bar{R}) = -\frac{1}{\rho} p_o + \bar{f}$$

where subscript "o" denotes quantities at equilibrium. Rewriting the cross product in the form of a gradient and using the dynamic condition on the free surface (8c):

$$\frac{p_o}{\rho} - \frac{1}{2}(\bar{\Omega}_o \times \bar{R})^2 - \bar{f} \cdot \bar{R} = \text{const.} \tag{15}$$

If the body force is a thrust $-g_o$ along the Z axis, then $\bar{f} \cdot \bar{R} = -g_o Z\bar{k}$, where $\bar{k}$ is a unit vector along z. The steady-state free surface equation becomes:

$$F_o(X,Y,Z) \equiv \frac{1}{2}\Omega_o^2(X^2 + Y^2) - g_o Z - C_o = 0$$

$F_o(X,Y,Z) = 0$ describes a paraboloid of revolution, where C_o is a constant that can be determined from the known fluid volume (Figure 2.)

Let η be the perturbation wave height in the direction normal to the free surface and (ζ,ρ) its components in the Z and R directions. Incrementing R by ρ and Z by ζ and retaining terms to the same order of smallness in (15),

$$\frac{p'}{\rho} = \Omega_o^2 R_x \rho - g_o \zeta \tag{16}$$

where p' is the perturbation free surface pressure. Let n_R and n_Z be the direction cosines of the unit normal to the free surface. Then (Figure 2),

$$\begin{aligned} n_R &= -\frac{1}{g_R}\frac{\partial F_o}{\partial R} = -\frac{\Omega_o^2 R_x}{g_R} \\ n_Z &= -\frac{1}{g_R}\frac{\partial F_o}{\partial Z} = \frac{g_o}{g_R} \\ g_R &= \sqrt{g^2 + (\Omega_o^2 R_x)^2} \end{aligned} \tag{17}$$

Substituting (17) in (16) and noting that

$$\eta = -\left(n_R \rho + n_Z \zeta\right)$$

we obtain the perturbed free surface boundary condition

$$\frac{p'}{\rho} = g_R \eta \tag{18}$$

By definition,

$$\dot{\eta} = \bar{n} \cdot \bar{u} \qquad \text{on } S_F \tag{19}$$

Substituting (14) in (19) using (13),

$$\dot{\eta} = -\bar{n} \cdot \nabla\phi = -\frac{\partial\phi}{\partial n} \tag{20}$$

(20) states that the perturbation velocity normal to the free surface results only from the potential ϕ, while $\bar{\psi}$ is purely geometric. Substituting (14) in (6) using (3) and (5),

$$\nabla\left\{-\frac{\partial\phi}{\partial t} - \frac{\partial\bar{\Omega}}{\partial t} \cdot \bar{\psi} + \frac{p}{\rho} - \bar{f} \cdot \bar{R} + \frac{1}{2}\bar{u}^2 + (\dot{\bar{\omega}} \times \bar{R}_o) \cdot \bar{r} - \frac{1}{2}(\bar{\Omega}_o \times \bar{R})^2\right\}$$

$$+ \frac{\partial\bar{\Omega}}{\partial t} \times \bar{r} + 2\bar{\Omega}_F \times \bar{u} = 0 \tag{21}$$

The physical meaning of each of the terms in (21) is elaborated in what follows:

$\frac{\partial\phi}{\partial t}$	unsteady translational potential satisfying the free surface boundary condition
$\frac{p}{\rho} - \bar{f} \cdot \bar{R}$	pressure and body forces
$\frac{1}{2}\bar{u}^2$	convective acceleration

$(\dot{\bar{\omega}} \times \bar{R}_o) \cdot \bar{r}$	perturbation tangential acceleration caused by rotation about the spin axis assuming that only translational oscillations are transmitted to the liquid
$\frac{1}{2}(\bar{\Omega}_o \times \bar{R})^2$	steady-state centrifugal acceleration
$\frac{\partial \bar{\Omega}}{\partial t} \times \bar{r}$	tangential acceleration from vortex oscillations
$2\bar{\Omega}_F \times \bar{u}$	total Coriolis acceleration from spin and vortex motions

In order to express the perturbation pressure at the free surface p' (equation 18) explicitly in terms of the ϕ, $\bar{\Omega}$, $\bar{\omega}$, and $\bar{\Omega}_o$, the terms

$$\dot{\bar{\Omega}} \times \bar{r} + 2\bar{\Omega}_F \times \bar{u} \tag{22}$$

are omitted in (21) so that the momentum equation may be expressed as an exact differential. That is,

$$\frac{p'}{\rho} \simeq \frac{\partial \phi}{\partial t} + \dot{\bar{\Omega}} \cdot \bar{\psi} - (\dot{\bar{\omega}} \times \bar{R}_o) \cdot \bar{r} \tag{23}$$

The neglect of the acceleration terms (22) is consistent with the linearized free surface condition (18). Eliminating p'/ρ from (18) and (23), we obtain the perturbed free surface boundary condition:

$$g_R \eta = \frac{\partial \phi}{\partial t} + \dot{\bar{\Omega}} \cdot \bar{\psi} + (\bar{r} \times \bar{R}_o) \cdot \dot{\bar{\omega}} \tag{24a}$$

Differentiating (24a) with respect to time and eliminating $\dot{\eta}$ using (20),

$$g_R \frac{\partial \phi}{\partial n} + \frac{\partial^2 \phi}{\partial t^2} \simeq -\ddot{\bar{\Omega}} \cdot \bar{\psi} - \left\{(\bar{\Omega}_o \times \bar{r}) \times \bar{R}_o\right\} \cdot \dot{\bar{\omega}}$$

$$- (\bar{r} \times \bar{R}_o) \cdot \ddot{\bar{\omega}} \tag{24b}$$

An approximate solution to the slosh problem can be found by adopting the Galerkin technique. A set of simple trial functions is sought

that satisy the boundary conditions of the irrotational problem (equation (24b) with $\bar{\Omega} = \bar{\omega} = 0$). A candidate set is composed of the eigenfunctions of the problem:

$$\begin{aligned} \nabla^2\phi_o &= 0 && \text{in } V \\ \frac{\partial\phi_o}{\partial n} &= 0 && \text{on } S_W \\ \frac{\partial\phi_o}{\partial n} + \frac{1}{g_R}\frac{\partial^2\phi_o}{\partial t^2} &= 0 && \text{on } S_F \end{aligned} \tag{25}$$

The eigenfunctions of problem (25) satisfy the orthogonality condition:

$$\int_{S_F} \frac{1}{g_R}\phi_m\,\phi_n dS = \delta_{mn}$$

where δ_{mn} is the Kronecker delta.

The functions ϕ and η in (24a) are expressed in terms of a truncated series in ϕ_n:

$$\begin{aligned} \phi(\bar{R}) &= \sum_{n=1}^{N} \lambda_n(t)\phi_n(\bar{R}) \\ \eta(\bar{R}) &= \sum_{n=1}^{N} \frac{1}{g_R}\xi_n(t)\phi_n(\bar{R}) \end{aligned} \tag{26}$$

Combining (20) and (25) using (26), we obtain:

$$\begin{aligned} \frac{\partial\phi}{\partial n} &= \sum_n \lambda_n \frac{\partial\phi_n}{\partial n} = \sum_n \frac{\sigma_n^2}{g_R}\lambda_n\,\phi_n \\ &= -\dot{\eta} = -\sum_n \frac{1}{g_R}\dot{\xi}_n\,\phi_n \end{aligned} \tag{27}$$

where $\{\sigma_n\}$ are the eigenfrequencies of problem (25).

Equation (27) yields to relations between ξ_n and λ_n

$$\dot{\xi}_n = -\sigma_n^2 \lambda_n \tag{28}$$

Substituting (26) and (28) in (24a),

$$\sum_{n=1}^{N} \left\{ \frac{1}{\sigma_n^2} \ddot{\xi}_n + \xi_n \right\} \phi_n = \dot{\bar{\Omega}} \cdot \bar{\psi} + (\bar{r} \times \bar{R}_o) \cdot \dot{\bar{\omega}} \tag{29}$$

Multiplying both sides of (29) by ϕ_n/g_R, integrating over the free surface, and using the orthogonality of the $\{\phi_n\}$ set,

$$\ddot{\xi}_n + \sigma_n^2 \xi_n = \sum_{i=1}^{N} (A_{in}\dot{\omega}_i + C_{in}\dot{\bar{\Omega}}_i)$$

$$\{A_{in}\} = -\frac{1}{\gamma_n} \left[\tilde{R}_o\right] \{b_{in}\}$$

$$\{C_{in}\} = \frac{1}{\gamma_n} \{a_{in}\}$$

$$\gamma_n = \int_{S_F} \phi_n^2/g_R dS \tag{30}$$

$$a_{in} = \int_S \psi_i \frac{\partial \phi_n}{\partial x_k} n_k \, dS = \int_S \phi_n \frac{\partial \psi_i}{\partial n} dS$$

$$= \int_S (\bar{r} \times \bar{n})_i \, \phi_n \, dS$$

$$b_{in} = \int_S x_i \frac{\partial \phi_n}{\partial x_k} n_k \, dS = \int_S \phi_n \frac{\partial x_i}{\partial x_k} n_k \, dS$$

$$= \int_S \phi_n \, n_i \, dS$$

$\left[\tilde{R}_o\right]$ is the skew symmetric tensor form of $\bar{R}_o$.

The total vorticity $\bar{\Omega}_F^*$ is governed by the Helmholz equation in rotating cordinates:

$$\frac{d\bar{\Omega}_F^*}{dt} + \bar{\Omega}_o \times \bar{\Omega}_F^* = (\bar{\Omega}_F^* \cdot \nabla)\,\bar{v}$$
$$\bar{\Omega}_F^* = \frac{1}{2}\nabla \times \bar{v} \qquad (31)$$

(31) can be derived by applying the curl operator to both sides of the momentum equation. In order to remove the spatial dependence, we define an average vorticity over the volume:

$$\bar{\Omega}_F = \frac{1}{V}\int_V \bar{\Omega}_F^*\, dV = \bar{\Omega} + \bar{\Omega}_o$$

Averaging equation (31),

$$\frac{d\bar{\Omega}_F}{dt} + \bar{\Omega}_o \times \bar{\Omega}_F \simeq \frac{1}{V}\int_V (\bar{\Omega}_F \cdot \nabla)\bar{v}\, dV \qquad (32)$$

The expression for $\bar{v}$ is found by combining (3) and (14):

$$\bar{v} = \bar{\omega}_R \times \bar{R}_o + \bar{\Omega}_F \times \bar{r} - \bar{\Omega} \cdot \nabla\bar{\psi} - \nabla\phi \qquad (33)$$

The gradient of the first two terms in (33) vanishes identically. The contribution of the third terms $\bar{v}^{(3)}$ is:

$$-(\bar{\Omega}_F \cdot \nabla)v_i^{(3)} = -\sum_{j=1}^{3} \Omega_j \frac{\partial}{\partial x_i}(\bar{\Omega}_F \cdot \nabla\psi_j)$$

Averaging throughout the volume and linearizing,

$$-\frac{1}{V}\int_V (\bar{\Omega}_F \cdot \nabla)v_i^{(3)}\, dV = -\sum_{j=1}^{3} \Omega_j R_{ij}$$

$$R_{ij} = \frac{1}{V}\int_V \frac{\partial}{\partial x_i}(\bar{\Omega}_F \cdot \nabla\psi_j)\, dV \qquad (34)$$

$$= \frac{1}{V}\int_S (\bar{\Omega}_F \cdot \nabla\psi_j)\, n_i\, dS \simeq \frac{\Omega_o}{V}\int_S \frac{\partial\psi_j}{\partial x_3} n_i\, dS$$

The linearized average of the fourth term $\bar{\bar{v}}^{(4)}$ can be expressed as:

$$\frac{1}{V}\int_V (\bar{\Omega}_F \cdot \nabla)\bar{v}^{(4)}\, dV = -\sum_{n=1}^{N} \frac{h_n \dot{\xi}_n}{\sigma_n^2} \tag{35}$$

$$\bar{h}_n = \frac{\Omega_o}{V}\int_V \frac{\partial}{\partial z}(\nabla\phi_n)\, dV = \frac{\Omega_o}{V}\int_S \frac{\partial \phi_n}{\partial z}\,\bar{n}\, dS$$

The linearized vector equation for homogeneous vorticity is then:

$$\dot{\bar{\Omega}} + (\bar{\bar{R}} + \tilde{\Omega}_o)\bar{\Omega} = \sum_{n=1}^{N} \frac{\bar{h}_n}{\sigma_n^2}\,\dot{\xi}_n \tag{36}$$

where $\bar{\bar{R}}$ is a tensor whose components are given by (34), $\bar{h}_n$ is the vector defined in (35), and $\tilde{\Omega}_o$ is the skew symmetric tensor of vector $\bar{\Omega}_o$.

The coupled equations given by (30) and (36) define the approximate rotational unsteady slosh motion of an ideal fluid with homogeneous vorticity in a spinning tank. The time history can be calculated once the truncated sets $\{\phi_n\}$ and $\{\sigma_n\}$ are determined.

IV. SLOSH FORCES AND MOMENTS

The slosh force and moment vectors ($\bar{F}$, $\bar{T}$), acting at the spacecraft reference point, are given by:

$$\bar{F} = \int_S p\bar{n}\, dS = \int_V \nabla p\, dV \tag{37}$$

$$\bar{T} = \int_S \bar{R} \times p\bar{n}\, dS = \int_V \bar{R} \times \nabla p\, dV \tag{38}$$

Using the expression for ∇p in (6) and the definitions of $\bar{\bar{u}}$ in (14),

$$\nabla p = -\rho\left\{\frac{\partial \bar{u}}{\partial t} + \frac{1}{2}\nabla \bar{u}^2 + \bar{\Omega} \times \bar{u} + 2\bar{\Omega}_o \times \bar{u} + \dot{\bar{\omega}}_R \times \bar{R}_o + \bar{\Omega}_o \times (\bar{\Omega}_o \times \bar{R}) - \bar{f}\right\} \tag{39}$$

$$\bar{u} = -\nabla\phi - (\bar{\Omega} \cdot \nabla)\bar{\psi} + \bar{\Omega} \times \bar{r}$$

$$\phi = -\sum_{n=1}^{N} \frac{1}{\sigma_n^2}\, \dot{\xi}_n\, \phi_n$$

$$\eta = \sum_{n=1}^{N} \frac{1}{g_R}\, \xi_n\, \phi_n$$

Substituting (39) in (37),

$$\bar{F} = M\left\{\bar{f} - \bar{\Omega}_o \times (\bar{\Omega}_o \times \bar{S})\right\} + M(\bar{R}_o \times \dot{\bar{\omega}})$$

$$- \sum_{n=1}^{N} \left\{\frac{\rho}{\sigma_n^2}\left(\bar{b}_n \ddot{\xi}_n + 2\bar{\Omega}_o \times \bar{b}_n \dot{\xi}_n + \sigma_n^2 \bar{d}_n \xi_n\right)\right\} \tag{40}$$

$$\bar{S} = \frac{1}{V}\int_V \bar{R}\, dV = \bar{R}_o + \bar{s} \quad \text{(fluid CG)}$$

$$b_{in} = \int_V \frac{\partial \phi_n}{\partial x_i}\, dV = \int_S \phi_n\, n_i\, dS$$

$$d_{in} = \int_{S_F} \phi_n\, n_i\, dS$$

The terms $M(\bar{f} - \bar{\Omega}_o \times (\bar{\Omega}_o \times \bar{S}))$ represent the equilibrium constant thrust and centrifugal body forces. The term $M(\bar{R}_o \times \dot{\bar{\omega}})$ is the translational force (constant throughout the fluid) generated by the perturbation angular acceleration $\dot{\bar{\omega}}$. The last bracket of (40) involves the slosh unsteady forces as it depends on the generalized coordinates ξ_n and their derivatives:

$\bar{b}_n \ddot{\xi}_n$ ⟶ translation inertia of slosh

$2\bar{\Omega}_o \times \bar{b}_n \dot{\xi}_n$ ⟶ Coriolis force due to relative velocity

$\bar{d}_n \xi_n \sigma_n^2$ ⟶ restoring force from potential energy

Note that the Coriolis effect is equivalent to a velocity proportional damping force. Substituting (39) in (38),

$$\bar{T} = M(\tilde{\bar{S}}\bar{f} + \tilde{\Omega}_o\bar{\bar{S}}\bar{\Omega}_o) + M\bar{\bar{S}}\dot{\bar{\omega}} + (\bar{\bar{B}} + \bar{\bar{A}})\dot{\bar{\Omega}} + 2(\bar{\bar{V}} - \bar{\bar{U}})\bar{\Omega} - \sum_{n=1}^{N} \frac{\rho}{\sigma_n^2}\left\{\left(\bar{a}_n + \tilde{R}_o\bar{b}_n\right)\ddot{\xi}_n + 2\bar{\bar{W}}_n\bar{\Omega}_o\dot{\xi}_n + \sigma_n^2\bar{f}_n\xi_n\right\} \qquad (41)$$

$\tilde{S}$ is the skew symmetric tensor of vector $\bar{S}$ in (40)

$$\bar{\bar{A}} = \rho\int_V \tilde{r}\,\tilde{r}\,dV$$

$$\bar{\bar{B}} = \rho\int_S r\,\bar{n}\,\tilde{\psi}^T\,dS$$

$$\bar{\bar{C}} = \rho\int_V \bar{r}\,\bar{r}^T\,dV$$

$$\bar{\bar{D}} = -\rho\Omega_o\delta_{j3}\int_V \tilde{r}\,(\nabla\psi_j)^{\sim}\,dV$$

$$\bar{\bar{F}}_n = -\int_V \tilde{r}(\nabla\phi_n)^{\sim}\,dV$$

$$a_n = \int_S \tilde{r}\,\bar{n}\,\phi_n\,dS \qquad \bar{e}_n = \int_{S_F} \tilde{r}\,\bar{n}\,\phi_n\,dS$$

$$\bar{b}_n = \int_S \bar{n}\,\phi_n\,dS \qquad \bar{g}_n = \int_{S_F} \bar{n}\,\phi_n\,dS$$

$$\bar{f}_n = \bar{e}_n + \tilde{R}_o\bar{g}_n \qquad S = \tilde{R}_o\tilde{R}_o + \tilde{s}\,\tilde{R}_o$$

$$\bar{\bar{U}} = \left[(M\,\bar{R}_o\,\bar{s}^T + \bar{\bar{C}})\,\bar{\Omega}_o\right]^{\sim} - M\,\tilde{R}_o\,\tilde{s}\,\tilde{\Omega}_o^T$$

$$\bar{\bar{V}} = \bar{\bar{D}} - M\,\tilde{R}_o\,\tilde{\Omega}_o\,\tilde{s}$$

$$\bar{\bar{W}}_n = \bar{\bar{F}}_n - \tilde{R}_o\,\tilde{b}_n$$

Quantities superscripted by ($^{=}$) are tensors, while ($^{\sim}$) denotes the skew symmetric matrix form of a vector. The first three moment terms in (41) result from the first three force terms in (40), while the ξ_n dependent contributions are born from the slosh unsteady forces. The $\dot{\bar{\Omega}}$ and $\bar{\Omega}$ dependent terms correspond to the couples produced by the vortex tangential acceleration and Coriolis acceleration, respectively.

V. PROCESS OF SOLUTION

The eignevalue problem (25) and the inhomogeneous potential problem $\bar{\psi}$ are solved using finite elements. Essentially, the fluid domain bounded by the sphere wall and the equilibrium free surface is subdivided into isoparametric finite elements. The Laplace equation and free surface boundary condition are written in a quadratic integral form:

$$I(\phi) = \frac{1}{2}\int_V (\nabla\phi)^2 dV - \frac{\lambda}{2}\int_{S_F} \frac{1}{g_R}\phi^2\, dS \tag{42a}$$

$$I(\psi_i) = \frac{1}{2}\int_V (\nabla\psi_i)^2 dV - \int_S (\bar{r}\times\bar{n})_i\psi_i\, dS \tag{42b}$$

The condition that the first variation of the functional in (42a) be stationary leads to the Laplace equation and free surface boundary condition in (25). A similar process on (42b) leads to the Laplace equation and inhomogeneous Neumann conditions of the potential $\bar{\psi}$.

The functional $I(\phi)$ can be discretized as:

$$I(\phi) = \sum_{k=1}^{M^*} I^{(k)}(\phi^{(k)}) \tag{43}$$

where M* is the total number of finite elements in the fluid volume V. Within each element, the field variable ϕ can be expressed in terms of its values at the nodal points using the interpolation functions $N_i^{(J)}(x,y,z)$:

$$\phi^{(k)}(x,y,z) = \sum_{i=1}^{n^*} N_i^{(k)}(x,y,z)\ \phi_i^{(k)} \tag{44}$$

n* denotes the number of nodes for some element and ϕ_i is the field variable at node i. The condition that the functional I be stationary is:

$$\delta I(\phi) = \sum_{j=1}^{M^*} \delta I^{(k)}(\phi^{(k)}) = 0$$

$$\frac{\partial I(\phi^{(k)})}{\partial \phi_i} = 0 \qquad i = 1,\ldots,n$$

Using (42a) and (44),

$$\sum_{j=1}^{n^*} \left\{ \int_V \left[\frac{\partial N_i}{\partial x}\frac{\partial N_j}{\partial x} + \frac{\partial N_i}{\partial y}\frac{\partial N_j}{\partial y} + \frac{\partial N_i}{\partial z}\frac{\partial N_j}{\partial z} \right] \right\} dV$$

$$-\lambda \int_{S_F} \left\{ \frac{N_i N_j}{g_R(R)}\, dS \right\} \phi_j = 0 \qquad \forall i,j$$

which can be written in matrix form for each element as:

$$\sum_{j=1}^{n^*} (A_{ij}^{(k)} - B_{ij}^{(k)})\phi_j = 0 \qquad \forall i,j$$

$$A_{ij}^{(k)} = \left(\frac{\partial N_i}{\partial x}\frac{\partial N_j}{\partial x} + \frac{\partial N_i}{\partial y}\frac{\partial N_j}{\partial y} + \frac{\partial N_i}{\partial z}\frac{\partial N_j}{\partial z} \right)_k \text{ over } V \qquad (45)$$

$$B_{ij}^{(k)} = \left(\frac{N_i N_j}{g_R} \right)_k \text{ on } S_F$$

where ϕ_j denotes the column vector of the nodal values ϕ_i. Furthermore, by splitting ϕ into ϕ_1 and ϕ_2, where ϕ_2 contains the free surface nodes only, (45) becomes:

$$\left[\begin{bmatrix} A_1 & A_2 \\ B_1 & B_2 \end{bmatrix} - \lambda \begin{bmatrix} 0 & 0 \\ 0 & B \end{bmatrix} \right] \begin{Bmatrix} \bar{\phi}_1 \\ \bar{\phi}_2 \end{Bmatrix} = 0$$

$$\Rightarrow \left[(B_2 - B_1 A_1^{-1} A_2) - \lambda B \right] \bar{\phi}_2 = 0 \qquad (46)$$

$$\bar{\phi}_1 = -A_1^{-1} A_2 \bar{\phi}_2$$

Applying the above procedure to the functional $I(\psi^{(k)})$ with the same interpolation functions $N_i(x,y,z)$ leads to a set of inhomogeneous simultaneous equations of the form:

$$\sum_{j=1}^{n} A_{ij}^{(k)} \psi_j = b_i^* \Rightarrow A\bar{\psi} = B^* \tag{47}$$

$A_{ij}^{(k)}$ is identical to the matrix in (45) and

$$b_i^* = \int_S (\bar{r} \times \bar{n})_i \, N_i \, dS$$

VI. SLOSH DAMPING SIMULATION

The energy dissipation associated with a sloshing liquid is governed by many complex processes that depend mainly on:

(a) Fluid kinematic viscosity

(b) Frequency and amplitude of excitation

(c) Tank geometry and fluid volume

(d) Ratio between centrifugal and thrust accelerations

To date, no theoretical investigation exists that models even qualitatively the damping mechanism (Ref.3-11). It is thought in this work that the problem is tractable only through empiricism that relies largely on experiment.

Summer and Stofan (Ref. 5) measured slosh forces on spherical tanks subjected to translational periodic motions of various amplitudes. The liquid kinematic viscosity ranged from 9.29×10^{-7} m^2/sec (10^{-5} ft^2/sec) for water to a maximum of 9.29×10^{-4} m^2/sec (10^{-2} ft^2/sec) for glycerine. For some fixed geometry and liquid properties, the nondimensional first mode slosh force $F_s/\rho g D^3$ was found to vary linearly with the excitation amplitude parameter X_o/D for small X_o/D, where

F_s = slosh force

ρ = liquid density

g = gravitational acceleration (or thrust)

D = tank diameter

X_o = amplitude of periodic excitation

A smooth transition region follows, beyond which the slosh force asymptotes to a constant value depending on liquid kinematic viscosity.

The observed trend can be explained as follows. For small amplitude vibrations, F_s is proportional to X_o as expected for a linear oscillator with constant proportional damping:

$$\Rightarrow F_s = C_F \rho g D^3 \frac{X_o}{D} \frac{1}{\sqrt{(\omega^2 - \omega_r^2)^2 + (2\zeta\, \omega\omega_r)^2}} ; \frac{X_o}{D} < O(1)$$

C_F = force coefficient function of geometry and fluid filling

ω, ω_r = excitation and resonant frequencies, respectively

ζ = equivalent viscous damping

ζ depends only on kinematic viscosity for linear motions. As the amplitude increases, free surface motions become nonlinear while the observed asymptotic behavior suggests that ζ is proportional to X_o/D ($\zeta \approx C_\zeta X_o/D$);

$$\Rightarrow F_s \approx C_F \rho g D^3 \frac{1}{2\omega\omega_r C_\zeta} ; \left(\frac{X_o}{D}\right)^2 > O(1)$$

It appears from the above limiting cases that the ζ variance with X_o/D is a hyperbola:

$$\zeta = \sqrt{\zeta_o^2 + \zeta_1^2 \left(\frac{X_o}{D}\right)^2} \tag{48}$$

An empirically derived expression for ζ_o is given in (Ref. 5) in the form:

$$\zeta_o = \frac{0.131}{2\pi} \left(\frac{\nu \times 10^4}{\sqrt{g D^3}}\right)^{0.359} f_h(h_a) \tag{49}$$

$$f_h(h_a) = \frac{1 + 0.46(2 - h_a)}{1.46(2 - h_a)} \quad \text{for } h_a \equiv \frac{h}{a} > 1$$

$$f_h(h_a) = \frac{a}{h} \quad \text{for } \frac{h}{a} \leq 1$$

h is the depth of the quiescent liquid in the tank.

In order to determine the dependence of ζ_1 on the liquid and geometric parameters, the steady-state slosh was computed for a periodic excitation corresponding to the fundamental slosh resonance in translation. A viscous damping term, proportional to the free surface normal velocity, was introduced in equation (30):

$$\ddot{\xi}_n + \underline{2\zeta \sigma_n \dot{\xi}_n} + \sigma_n^2 \xi_n = f(\dot{\bar{\omega}}, \bar{\Omega}, \dot{\bar{\Omega}}) \tag{50}$$

The damping factor ζ was varied until a numerical value of the slosh force F_s coincided with the experimental value. A hyperbola was then fitted to the resulting $\{\zeta, X_o/D\}$ set in the form:

$$\zeta = \sqrt{\zeta_o^2 + 10(1 + 2\pi\zeta_o)\left(\frac{X_o}{D}\right)^2} \tag{51}$$

The frequency response spectrum was computed for a periodically excited spherical tank based on the damping factor expression (51). The geometric and liquid characteristics were:

$a = 18.4$ cm (7.25 in.) $\qquad \frac{h}{D} = 0.5$

$\rho = 1000$ kg/m^3 (62.2 lb/ft^3) $\qquad \frac{X_o}{D} = 0.0083$

$0.5 \leq \eta^* \leq 2.0 \qquad g = 9.81$ m/sec^2 (32.2 ft/sec^2)

η^* is the nondimensional frequency parameter

$$\eta^* = \omega\sqrt{\frac{a}{g}}$$

Figure 3 compares the present analysis with test data from Ref. 12. The correlation is satisfactory up to $\eta^* = 1.3$ just after the fundamental slosh resonance. Beyond this point, the analysis tends to underestimate the slosh force, while the error increases uniformly with frequency. A possible explanation for this discrepancy is given in what follows.

Liquid slosh in spherical tanks falls in one of four different regimes:

(1) At low frequencies ($\eta^* \leq 1.1$) the small amplitude free surface motion is in phase with the excitation. The liquid is mainly acted upon by slug forces (externally applied translational accelerations). The response is very similar to that of a

linear damped single degree of freedom oscillator having a mass equal to the total fluid mass.

(2) As the frequency increases beyond $\eta^* = 1.1$, the fundamental resonance is approached. This results in an increase of the liquid mobility (degrees of freedom) and greater free surface amplitude. The slosh wave is broken down into small drops as a result of splashing against the tank wall. In addition, it froths due to surface cavitation and release of entrained vapor. These phenomena are associated with an appreciable increase in energy loss that is considerably higher than that in the linear regime.

(3) Beyond the first resonance ($\eta^* \geq 1.25$), the excitation and response are out of phase. This leads to an increase in relative velocity between the slosh wave and the solid boundary. Breaking of the slosh wave as it follows the adverse slope of the wall occurs whenever the tank is more than 40% full and the wave amplitude is sufficiently large.

It is believed that the dissipation mechanism is far more complex in the case of a spinning tank. Experiments were conducted at Hughes Aircraft in 1972 (Ref. 13) on a spinning table supported by an air bearing. The measured rate of energy dissipation from slosh was found orders of magnitude higher than that predicted analytically. In fact, the energy dissipation from slosh has destabilizing effects for a certain range of the ratio between spin and transverse inertias of the spacecraft.

VII. NUMERICAL RESULTS

Since the resultant gravitational acceleration g_R enters as a parameter in the definition of the nondimensional frequencies, a value $g_R = 9.81$ m/sec^2 was assumed throughout the computations while the angle β:

$$\beta = \tan^{-1}\left\{\frac{(R_{ox} + s_x)\Omega_o^2}{g}\right\}$$

was varied by changing both thrust g and spin rate Ω_o for a mixed geometery and fluid volume. The "Galileo" tank was assumed with the following parameters:

$$a = 0.37 \text{ m}$$

$$R_{ox} = 0.64 \text{ m}$$

$$\rho = 872 \text{ kg/m}^3 \qquad \text{(light-fluid)}$$

$$\nu = 0.277 \times 10^{-6} \text{ m}^2/\text{sec}$$

$$V_{liquid}/V_{tank} = 0.5$$

The tank was spun to a constant rate (Ω_o) on a rigid platform with a superimposed periodic excitation about the spin axis such that the equivalent maximum oscillatory amplitude at the center of the tank was always one percent of the tank diameter ($X_o/D = 0.01$). Thus,

$$\bar{\omega} = \omega_o \sin \omega t \, \bar{k}$$

$$\omega_o = 0.01 \frac{\omega D}{R_{ox}}$$

where ω_o and ω are the excitation amplitude and frequency, respectively.

Table 1 shows three test cases in the β range of interest.

The variation of steady-state nondimensional circumferential force $Fy/(\rho g_R D^3 X_o/D)$ with frequency parameter η^* for the three cases in Table 1 are shown Figures 4,5, and 6. As expected, case A (no spin) exhibits one resonance at $\eta^* = 1.25$. A similar behavior is noticed for case C (no thrust) except that the resonance occurs at a lower $\eta^* = 1.04$. The response for case B is different in that three resonances are encountered. The first resonance is associated with a vortex dominant motion. The next two resonance correspond to mostly potential irrotational modes about two orthogonal axes on the free surface. A weak fourth resonance can be detected at $\eta^* = 1.6$ and relates to the slosh mode with two circumferential nodes at the free surface.

In the process of numerical experiments, a slosh instability was detected fluid fills $\tilde{V} = (V_{fluid}/V_{tank})$ less than 0.55. The exponential instability was found to exist in a range of β angles that depends on the fluid fill $\tilde{V}$. The range is largest at the lower $\tilde{V}$ and decreases

Table 1. Representative test cases

Case	V_{liquid}/V_{tank}	Ω_o, RPM	g, m/s^2	g_R, m/s^2	β, Deg
A	0.5	2.0	9.81	9.81	0.01
B	0.5	31.5	5.50	9.81	52
C	0.5	34.0	0.0	9.81	90

uniformly as $\tilde{V}$ increases to a $\tilde{V}$ of 0.55, beyond which the instability vanishes. The stability boundary (Figure 7) is independent of the resultant gravitational acceleration g_R.

The unexpected occurrence of the instability suggested further investigation into its nature and mechanism. The complex characteristic eigenvalues of the governing system of linear differential equations (30) and (36) were determined for different $\tilde{V}$ in the range $0 \leq \beta \leq$ 90 deg. The variation of the nondimensional imaginary roots representing the frequencies and their corresponding nondimensional real parts representing the damping is plotted versus β in Figures 8 through 14 with $\tilde{V}$ as a parameter. For low $\tilde{V}$ (nearly empty tank) the first frequency vanishes at $\beta = 0$, then rapidly increases to coalesce with the second resonance in the range of instability. The two frequencies then separate once more in the stable regime, while the lowest frequency approaches a finite value as β reaches 90 deg. The damping associated with the first frequency starts at zero for $\beta = 0$, while that corresponding to the second frequency is finite. As the instability region is approached, the first mode damping assumes larger negative values, while the second mode becomes overly damped. This behavior ceases as we exit the instability range. The frequency separation between the first two modes increases uniformly with fluid fill $\tilde{V}$, an indication of a weaker instability. The dashed lines represent the first two resonances of the approximate eigenvalue problem (25). The different negative damping parameters of the first mode are plotted against β with $\tilde{V}$ as a parameter in Figure 15.

The phenomenon bears resemblance to aeroelastic flutter in which the bending and torsional elastic wing frequencies coalesce (Ref. 14). In the present model, the vortex and irrotational slosh frequencies couple in a manner similar to the wing frequencies in flutter.

VIII. STABILITY ANALYSIS OF FREE SLOSHING

A separate stability analysis on the "free-slosh" equations was performed for all cavity fill ratios and all values of $0 \leq \beta \leq 90$ deg.

Consider Euler's equation for fluid motion in a rotating system (Eq. 6 with $\bar{\omega} = \dot{\bar{\omega}} \equiv 0$) with homogeneous boundary conditions given by (8a,b,c). The steady-state solution is given by (15).

Let $\bar{v}(\underline{x},t)$ be the infinitesimal perturbational velocity of the fluid, and $p_1(\underline{x},t)$ be the infinitesimal perturbational pressure. Then, using (6) and (15), the equation of perturbed motion of the fluid is:

$$\frac{\partial \bar{v}}{\partial t} + 2\bar{\Omega} \times \bar{v} = -\frac{1}{\rho} \nabla p_1 \qquad (52)$$

$$\nabla \cdot \bar{v} = 0 \qquad \text{in } V_o$$

Outside of V_o there is a "gravitational field" $\bar{g}_e$ given by:

$$\bar{g}_e = \omega^2[x\bar{i} + y\bar{j}] = g\bar{k} \tag{53}$$

As a result of the perturbed motion, the free surface is perturbed. Let the elevation of the perturbed free surface relative to the equilibrium free surface S_{F_o} be denoted by ζ, measured normal to S_{F_o}.

From (15) and (53) it is easily seen that $\bar{g}_e$ is normal to the free surface, and is directed into the fluid.

As before,

$$\bar{v} \cdot \bar{n} = 0 \qquad \text{on } S_{W_o}$$

The pressure on the equilibrium free surface S_{F_o} is given by:

$$p_1 \Big|_{S_{F_o}} = \rho \bar{g}_e \cdot \bar{n} \zeta \qquad \text{on } S_{F_o} \quad \text{(correct to } O(\zeta))$$

Consider the Liapunov functional (Ref. 15):

$$L = \frac{1}{2} \int_{V_o} \rho \, \bar{v} \cdot \bar{v} \, dV_o + \frac{1}{2} \rho \, g_e \int_{S_{F_o}} \zeta^2 \, d S_{F_o} \tag{54}$$

$$g_e = \bar{g}_e \cdot \bar{n}$$

Consider the time derivative of L:

$$\dot{L} = \int_{V_o} \rho \, \bar{v} \cdot \frac{\partial \bar{v}}{\partial t} \, dV_o + \int_{S_{F_o}} \rho \, g_e \, \zeta \frac{\partial \zeta}{\partial t} \, d S_{F_o} \tag{55}$$

Using (52) in (55):

$$\dot{L} = -\int_{V_o} \rho \left(2 \Omega \times \bar{v} \cdot \bar{v} + \frac{1}{\rho} \bar{v} \cdot \nabla p_1\right) dV_o + \int_{S_{F_o}} \rho \, g_e \, \zeta \frac{\partial \zeta}{\partial t} \, dS_{F_o}$$

Using the divergence theorem on the remaining terms in the first integral (note $\bar{\Omega}\times\bar{V}\cdot\bar{V} = 0$),

$$\dot{L} = -\int_{V_o} p_1 \nabla\cdot\bar{v}\, dV_o - \int_{S_{F_o}} p_1\, \bar{v}\cdot\bar{n}\, dS_{F_o} - \int_{S_{W_o}} p_1\, \bar{v}\cdot\bar{n}\, dS_{W_o} + \int_{S_{F_o}} \rho g_e \zeta \frac{\partial\zeta}{\partial t} dS_F$$

Now

$$\nabla\cdot\bar{v} = 0 \text{ in } V_o; \quad \bar{v}\cdot\bar{n} = 0 \text{ on } S_{W_o}; \quad \bar{v}\cdot\bar{n} = \frac{\partial\zeta}{\partial t} \text{ on } S_{F_o}$$

$$p_1 = \rho g_e \zeta \text{ on } S_{F_o}$$

Hence, $\dot{L} = 0$. Thus, the functional

$$L = \frac{1}{2}\int_{V_o} \rho\, \bar{v}\cdot\bar{v}\, dV_o + \frac{1}{2}\int_{S_{F_o}} g_e \rho\, \zeta^2\, dS_{F_o}$$

is conserved in free sloshing. Therefore, free sloshing is stable (marginally stable).

This proves the assumption of homogeneous vorticity is invalid for problems of free sloshing and, therefore, by implication, for problems of forced sloshing.

REFERENCES

1. Pfeiffer, F., "Ein Naeherungsverfahren fuer Fluessigkeitsgefuellte Kreisel," Ingenieur, Archiv 43, 1974, pp. 306-316.

2. Lamb, H., "Hydrodynamics," Dover Publications, 6th Edition, 1932.

3. Stephens, David G., Leonard, H. Wayne, and Silveira, Milton A., "An Experimental Investigation of the Damping of Liquid Oscillations in an Oblate Spheroidal Tank With and Without Baffles," NASA TN D-808, 1961.

4. Stephens, David G., Leonard, H. Wayne, and Perry, Tom W., "Investigation of the Damping of Liquids in Right-Circular Cylindrical Tanks Including the Effects of a Time-Variant Liquid Depth," NASA TN D-1367, 1962.

5. Summer, Irving E., and Stofan, Andrew J., "An Experimental Investigation of Viscous Damping of Liquid Sloshing in Spherical Tanks," NASA TN D-1991, 1963.

6. Mikishev, G. N., and Dorozhkin, N. Ya, "An Experimental Investigation of Free Oscillations of a Liquid in Containers (in Russian)," Izv. Akad, Nauk SSSR, Otd. Tekh. Nauk, Mekh. i Mashinostr, No. 4, July/Aug. 1961, pp. 48-83.

7. Abramson, H. Norman, Chu, Wen-Hwa, and Garza, Luis R., "Liquid Sloshing in Spherical Tanks," AIAA J., Vol. 1, No. 2, Feb. 1963, pp. 384-389.

8. Williams, D. D., "Estimates of Energy Dissipation and Nutation Damping Due to Fuel Sloshing in a Spherical Tank," Hughes IDC 2280.03/202, 1 June 1965.

9. Porter, W. W., "Fuel Slosh Damping Test with ATS Tanks and Test Fixture," Hughes IDC 223/2466, May 12, 1970.

10. Edwards, R. H., "Fuel Damping of Intelsat IV," Hughes IDC 2245.2/8, May 9, 1969.

11. Neer, J. T., "Intelsat IV Fuel Slosh Dissipation Rates and Time Constants," Hughes IDC HS312-2286-3-F161, Feb. 13, 1970.

12. Abramson, N., "The Dynamic Behaviour of Liquids in Moving Containers," NASA SP-106, 1966.

13. Neer, J., "Fuel Slosh Energy Dissipation on a Spinning Body," Hughes Aircraft Co., El Segundo, Feb. 1972.

14. Roccard, Y., "Dynamique Générale des Vibrations," Deuxième Edition, Masson et Cie, Paris, 1949.

15. Caughey, T. K., "Review of Galileo Slosh," Interoffice Memorandum, June 15, 1979 (JPL internal document).

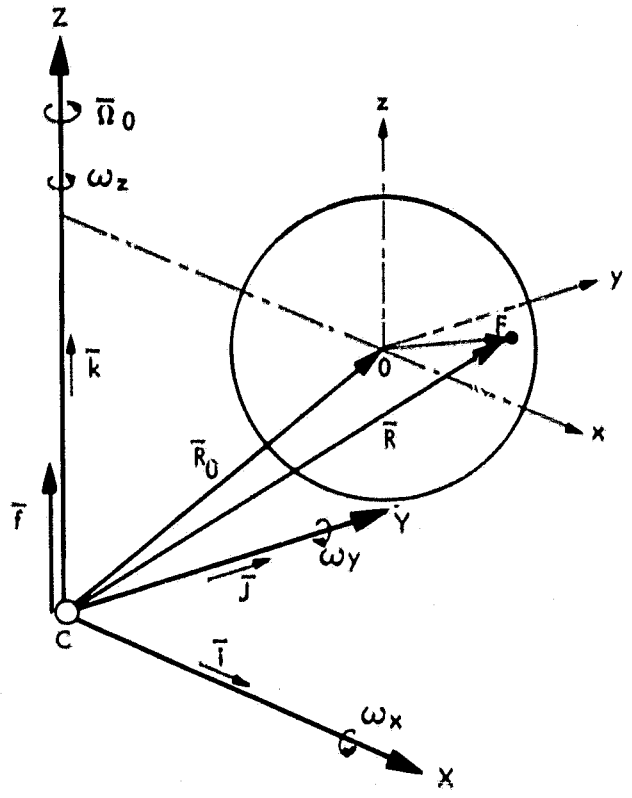

Figure 1. Reference and local rotating coordinate systems

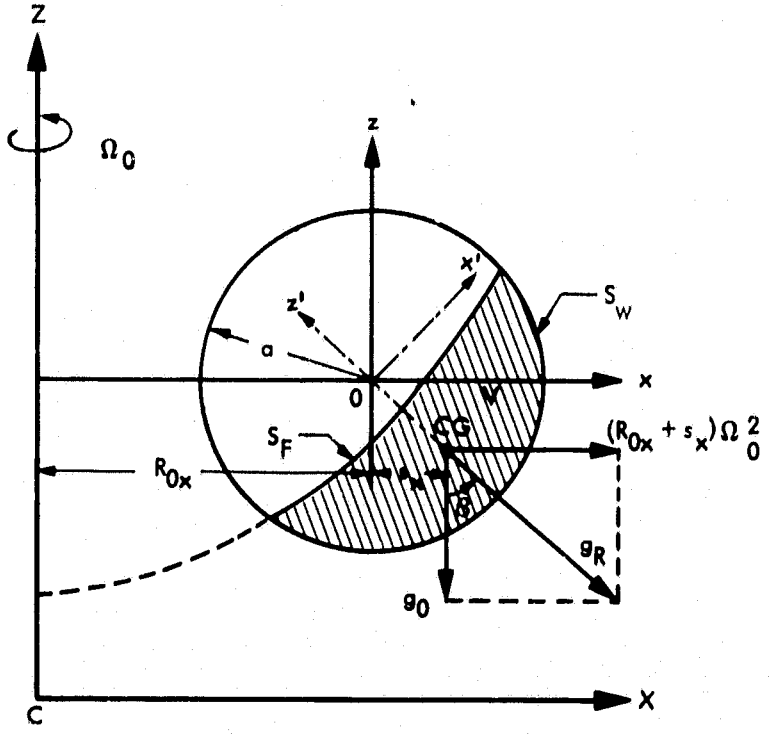

Figure 2. Accelerations on fluid volume

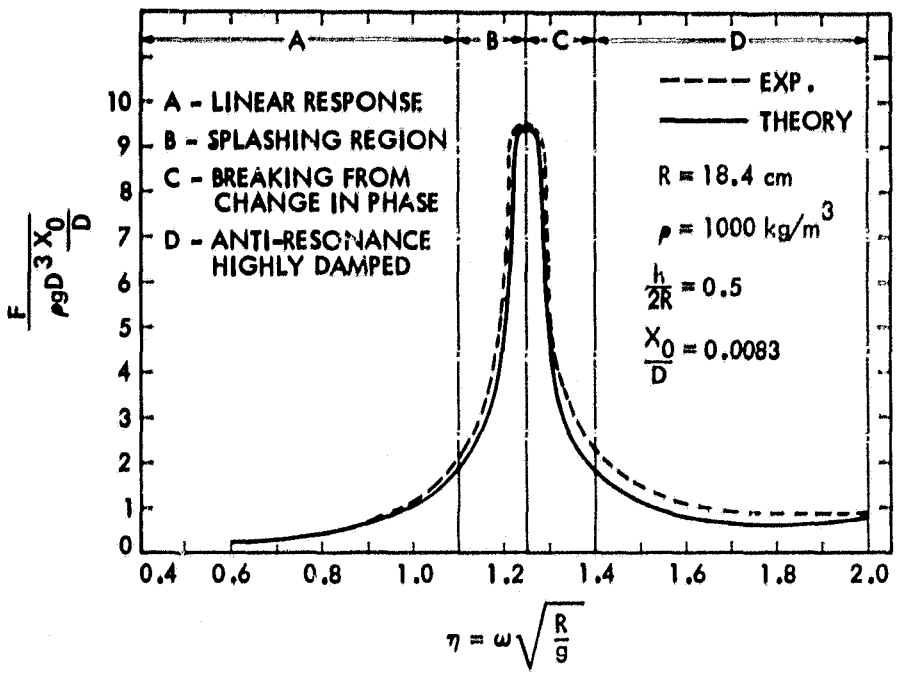

Figure 3. Comparison for translational slosh

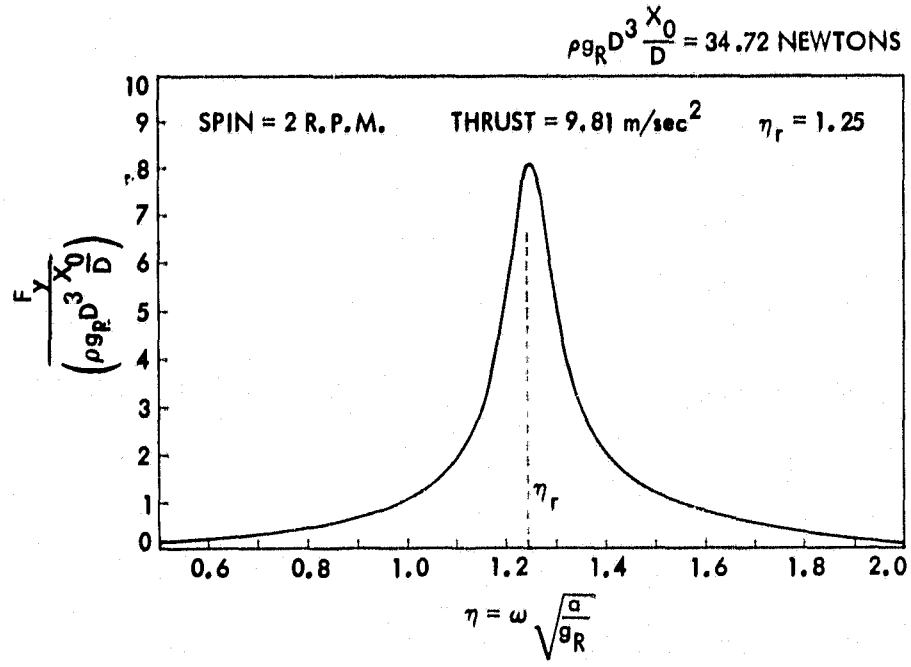

Figure 4. Nondimensional tangential slosh force for case A

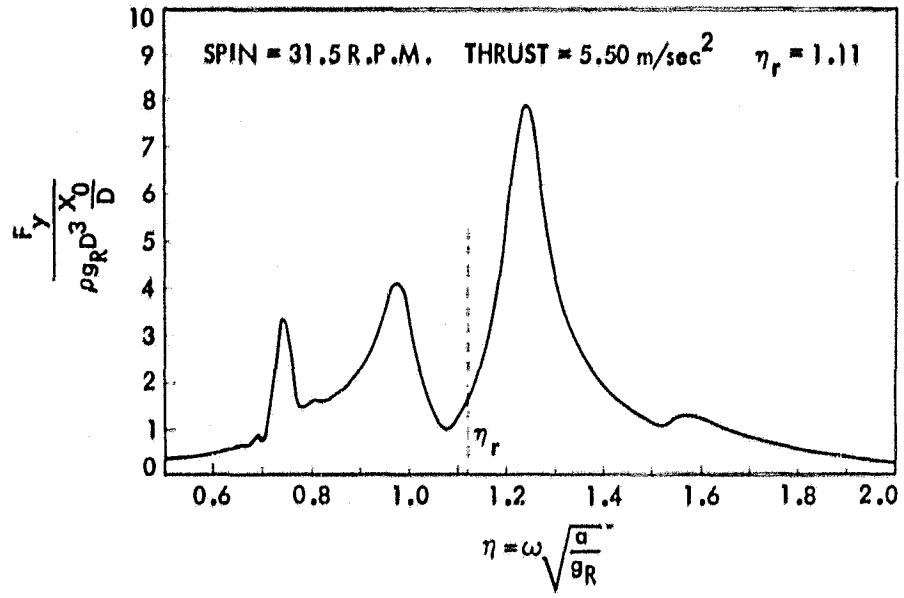

Figure 5. Nondimensional tangential slosh force for case B

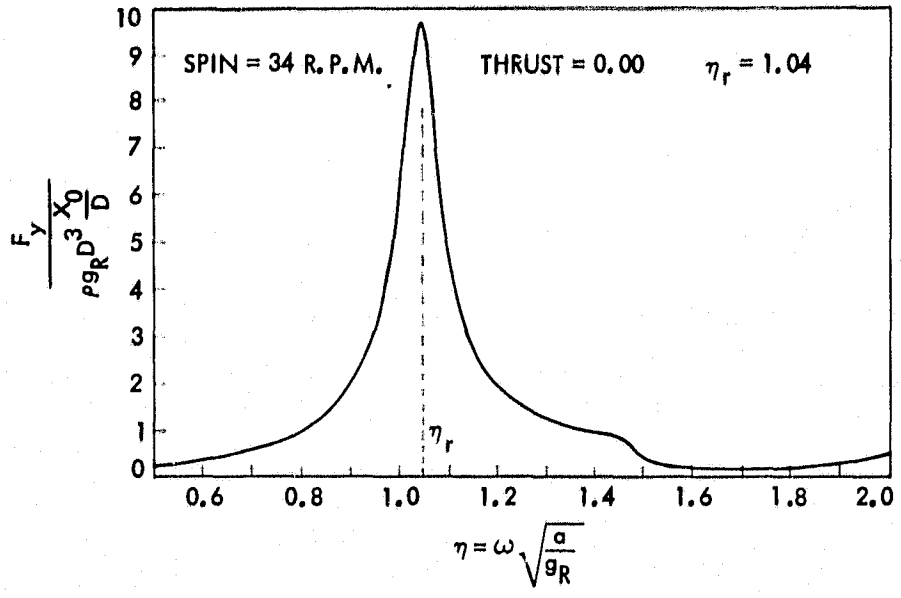

Figure 6. Nondimensional tangential slosh force for case C

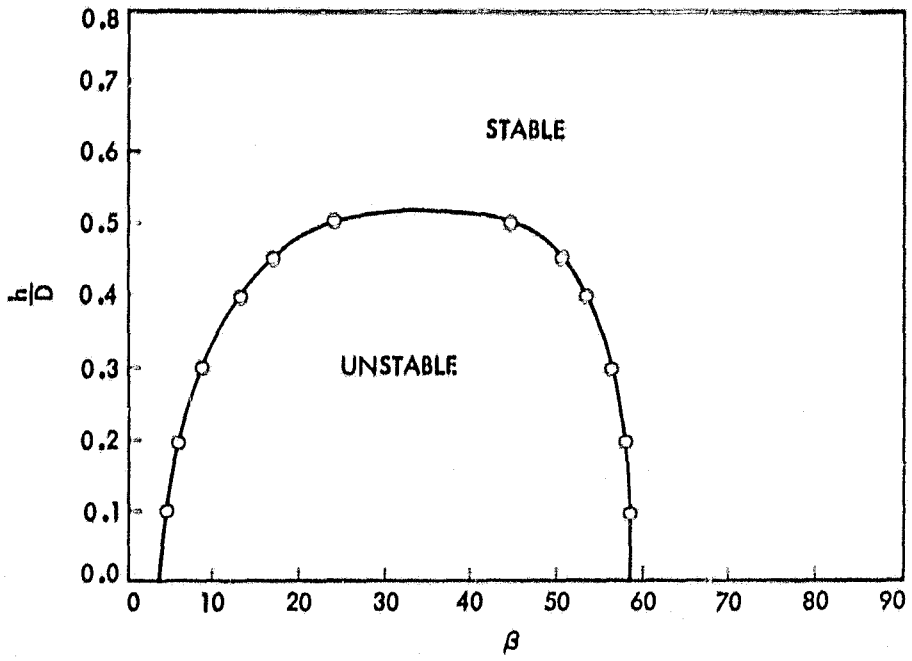

Figure 7. Stability boundary

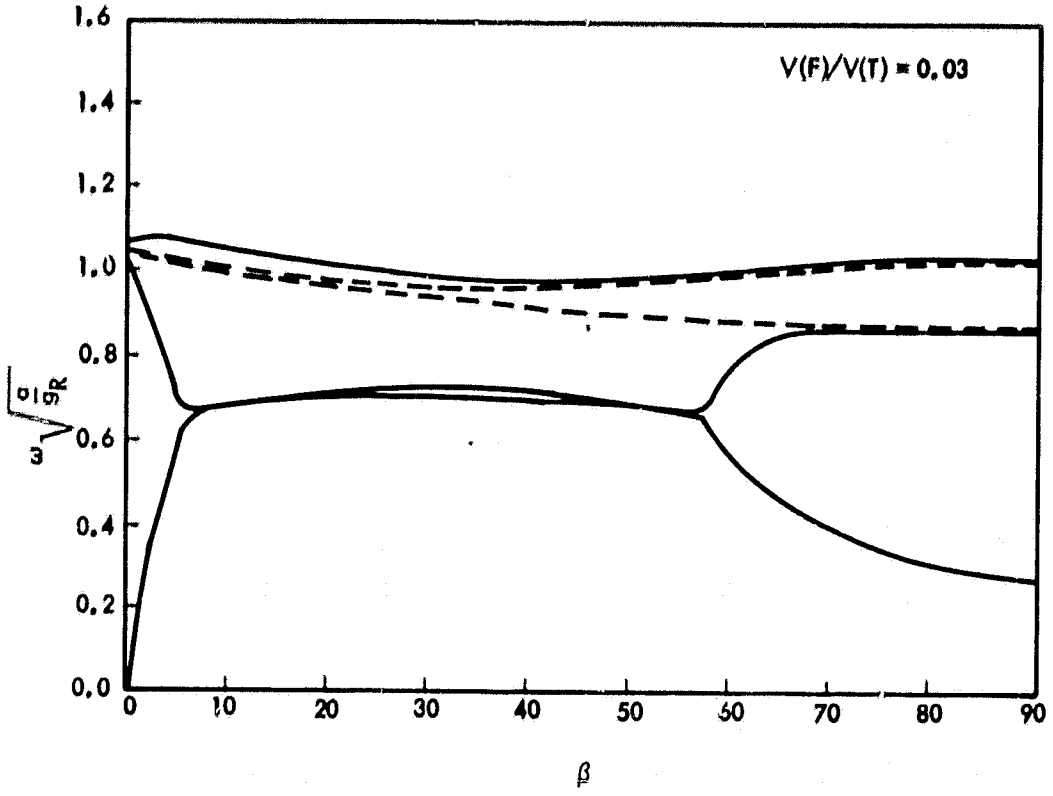

Figure 8a. Characteristic frequencies for $\tilde{V}$ = 0.03

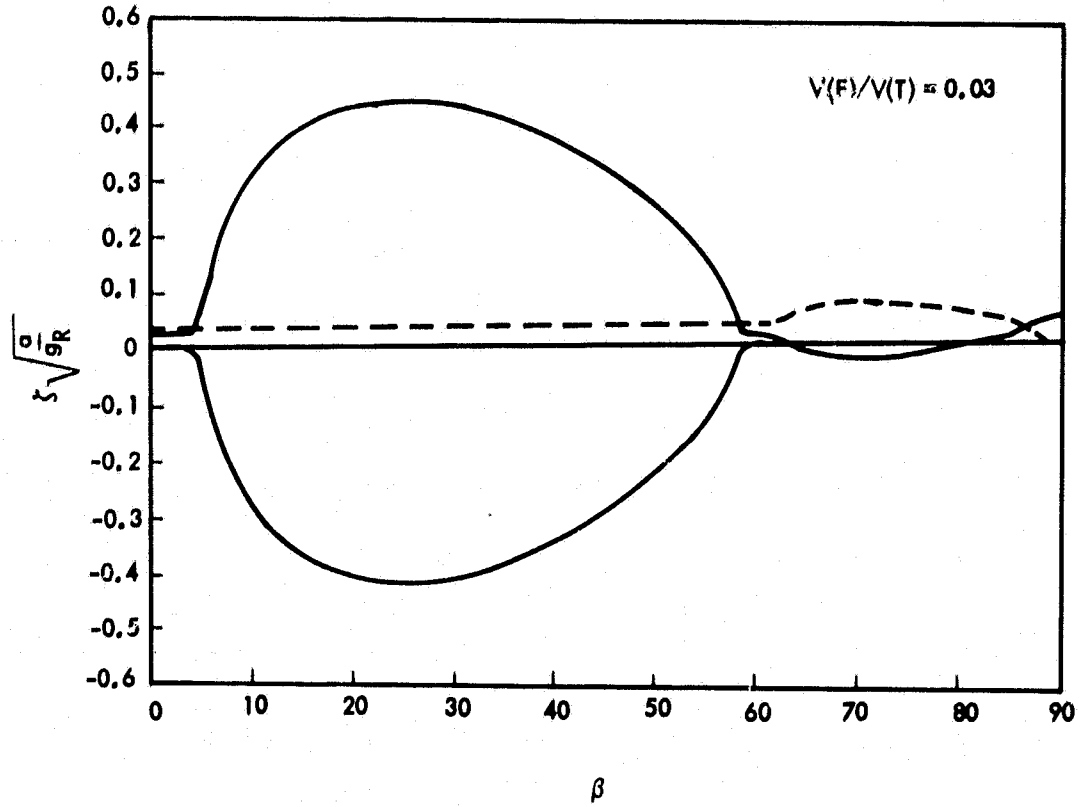

Figure 8b. Characteristic damping for $\tilde{V}$ = 0.03

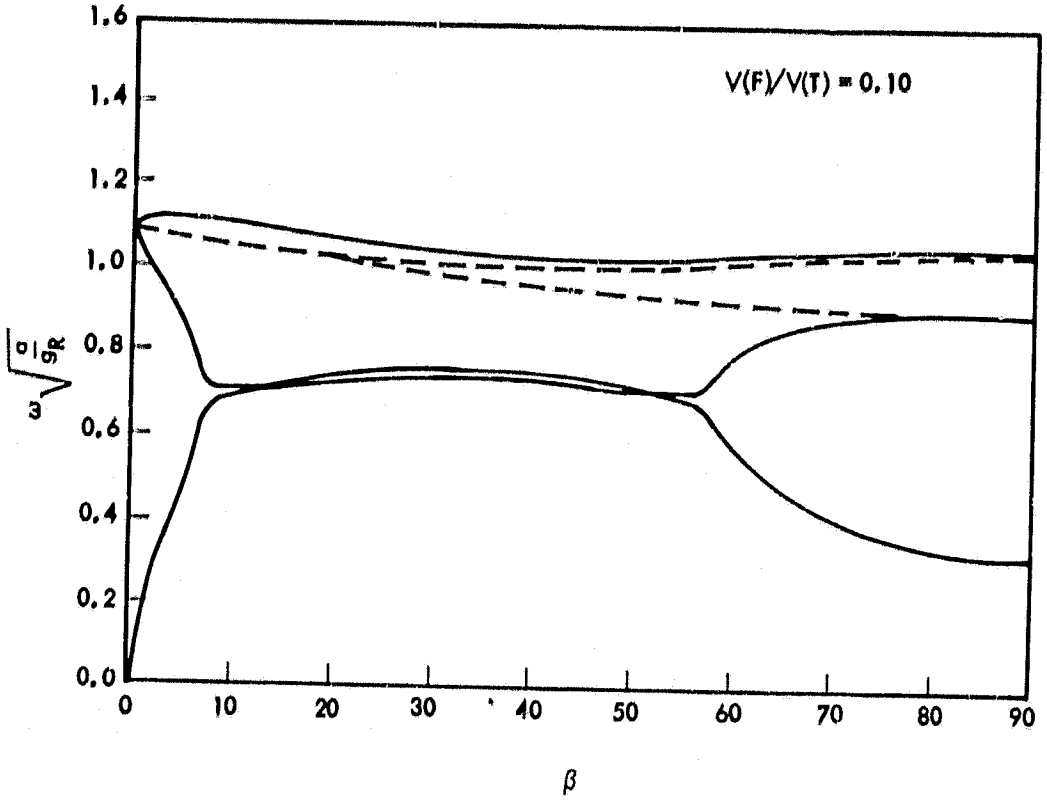

Figure 9a. Characteristic frequencies for $\tilde{V} = 0.10$

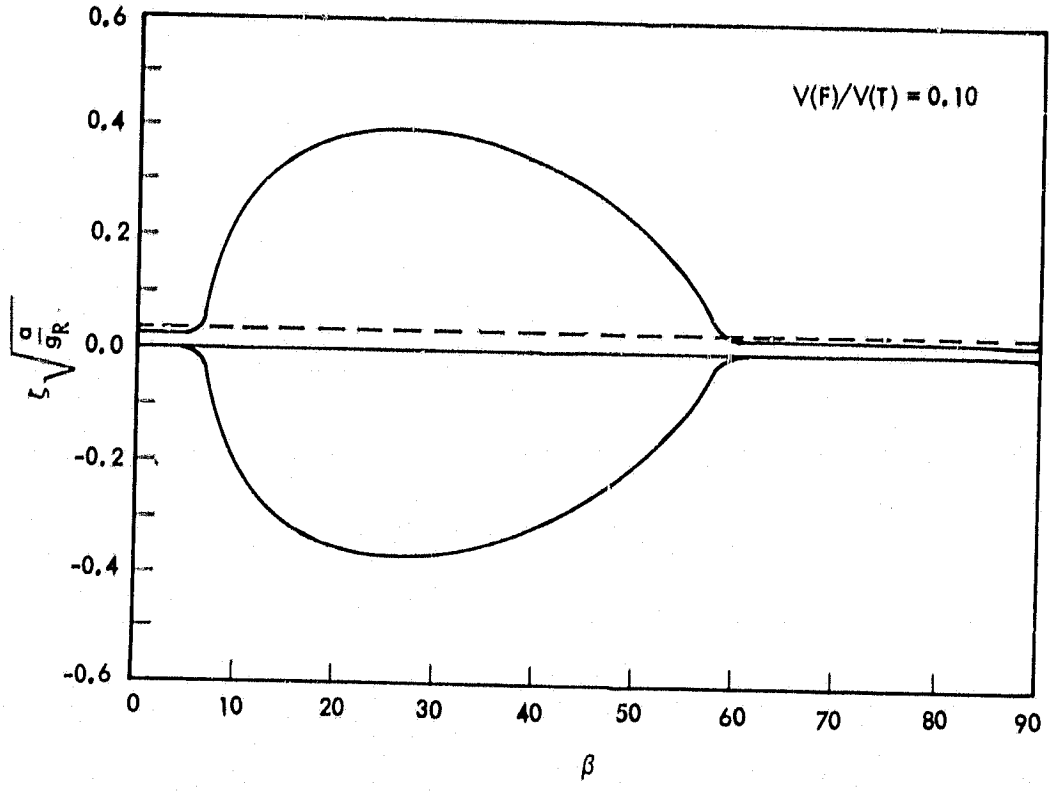

Figure 9b. Characteristic damping for $\tilde{V} = 0.10$

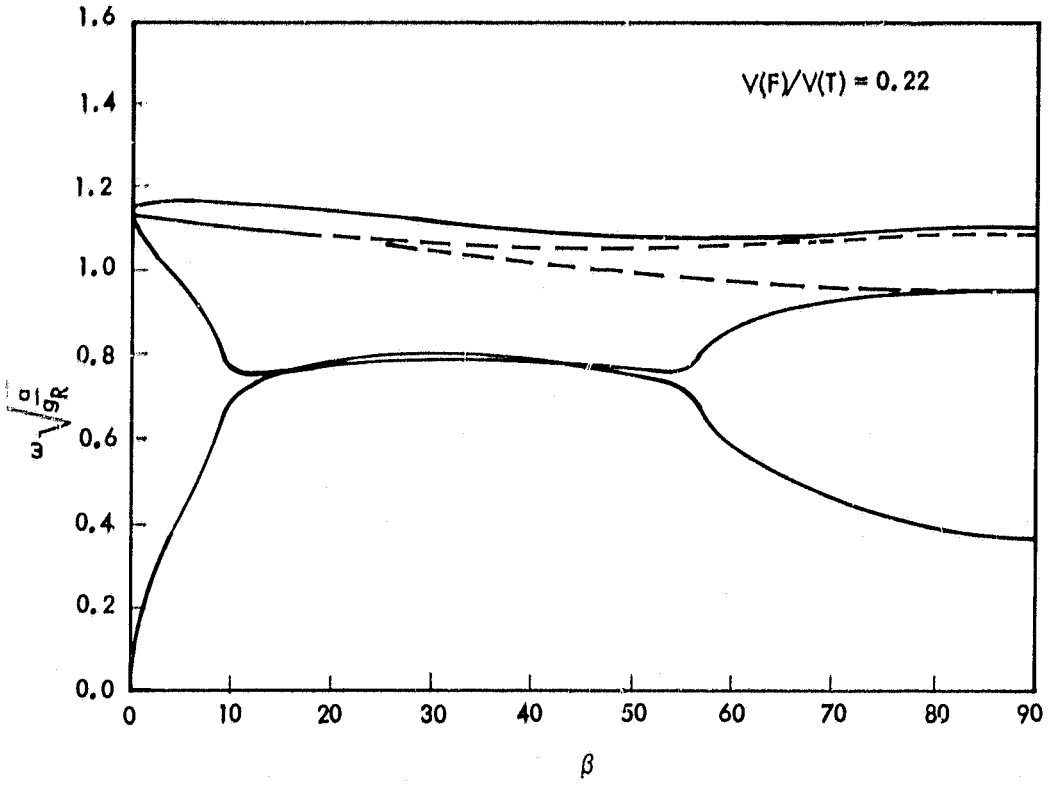

Figure 10a. Characteristic frequencies for $\tilde{V}$ = 0.22

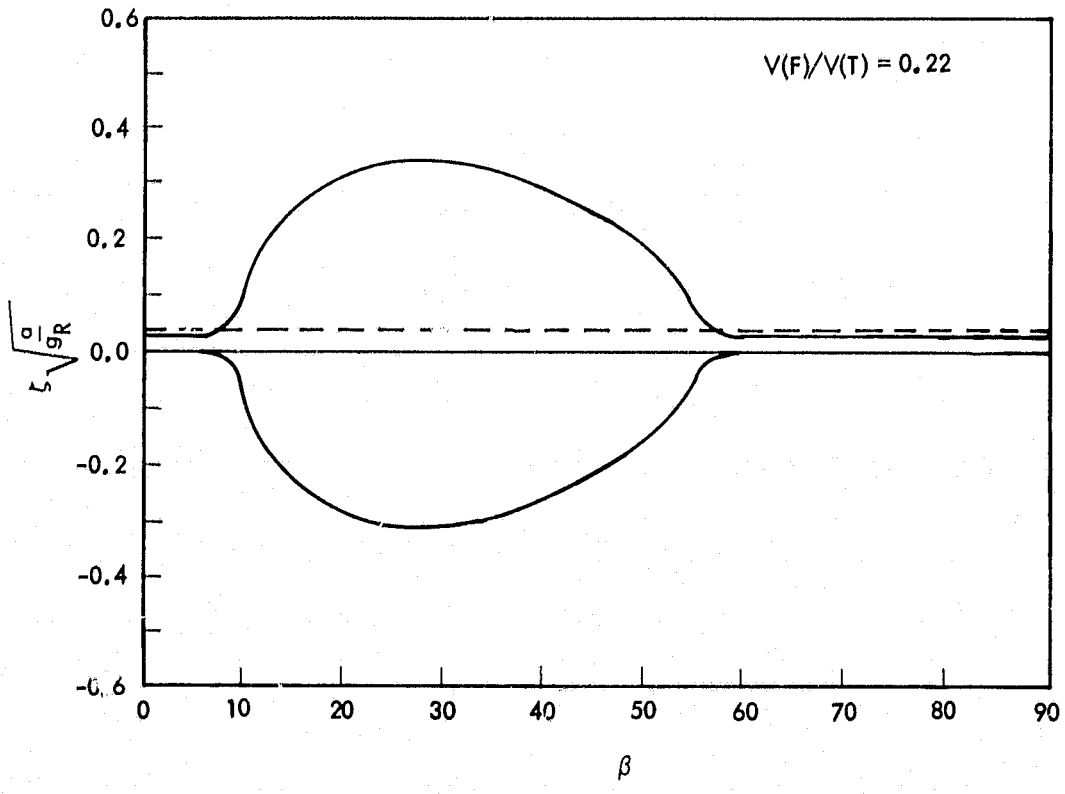

Figure 10b. Characteristic damping for $\tilde{V}$ = 0.22

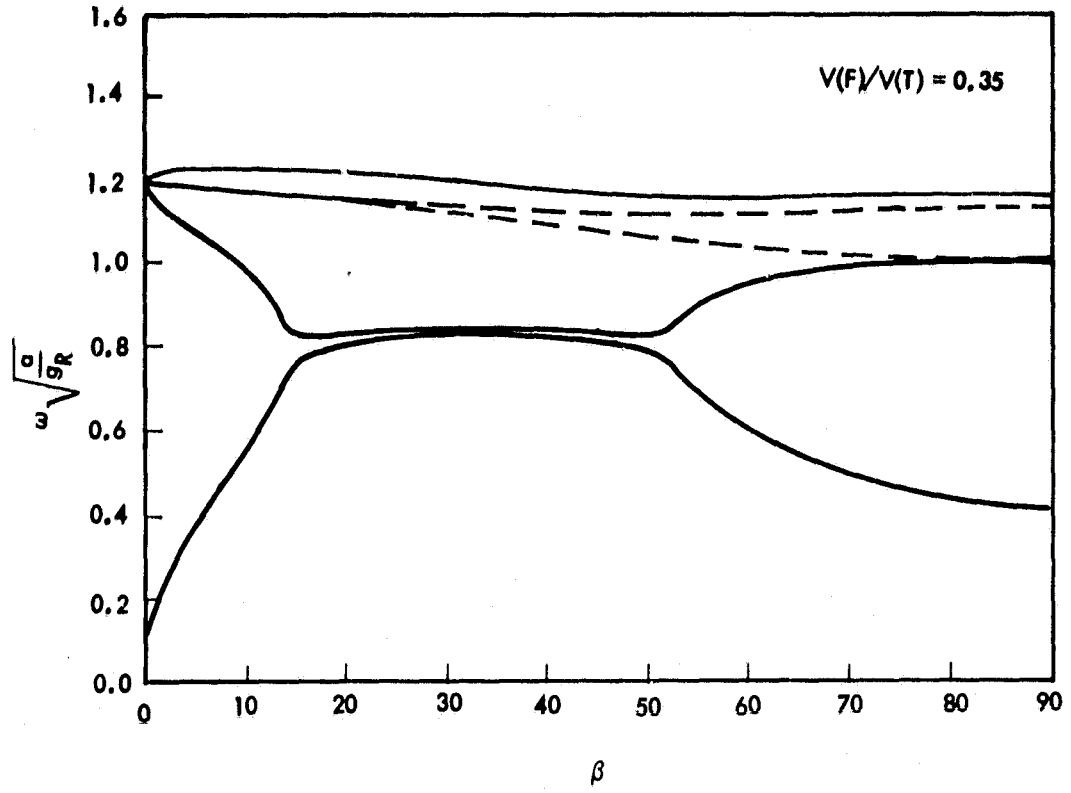

Figure 11a. Characteristic frequencies for $\tilde{V}$ = 0.35

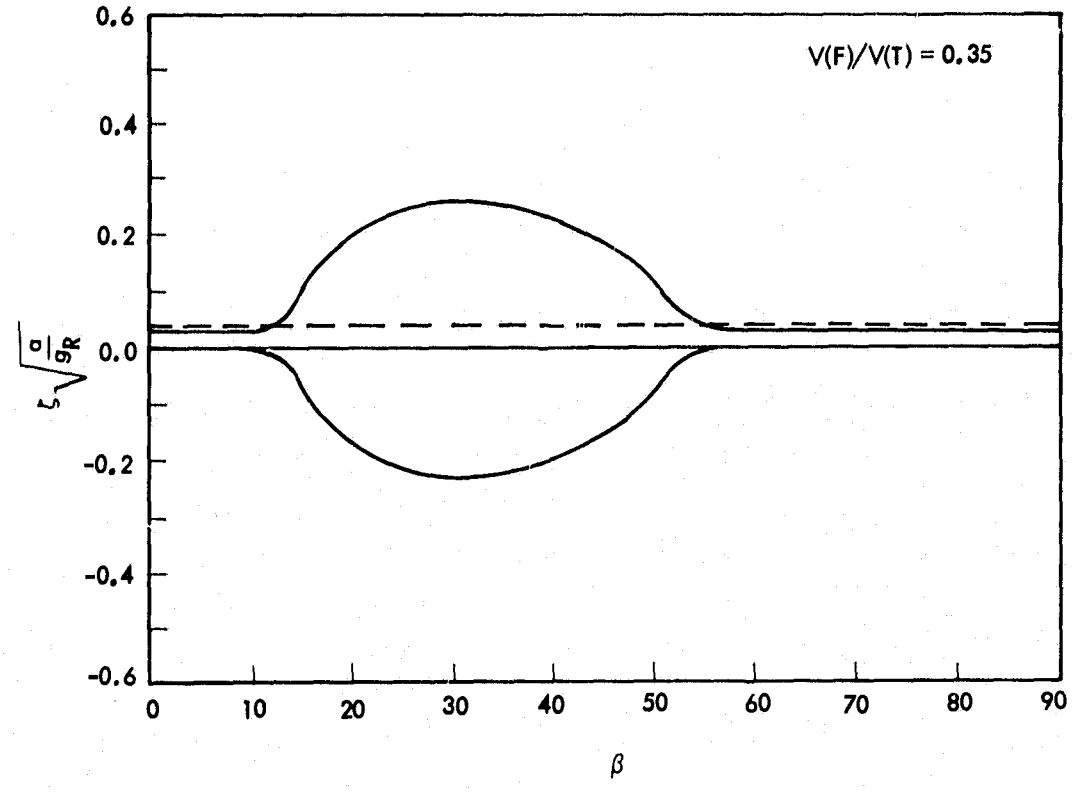

Figure 11b. Characteristic damping for $\tilde{V}$ = 0.35

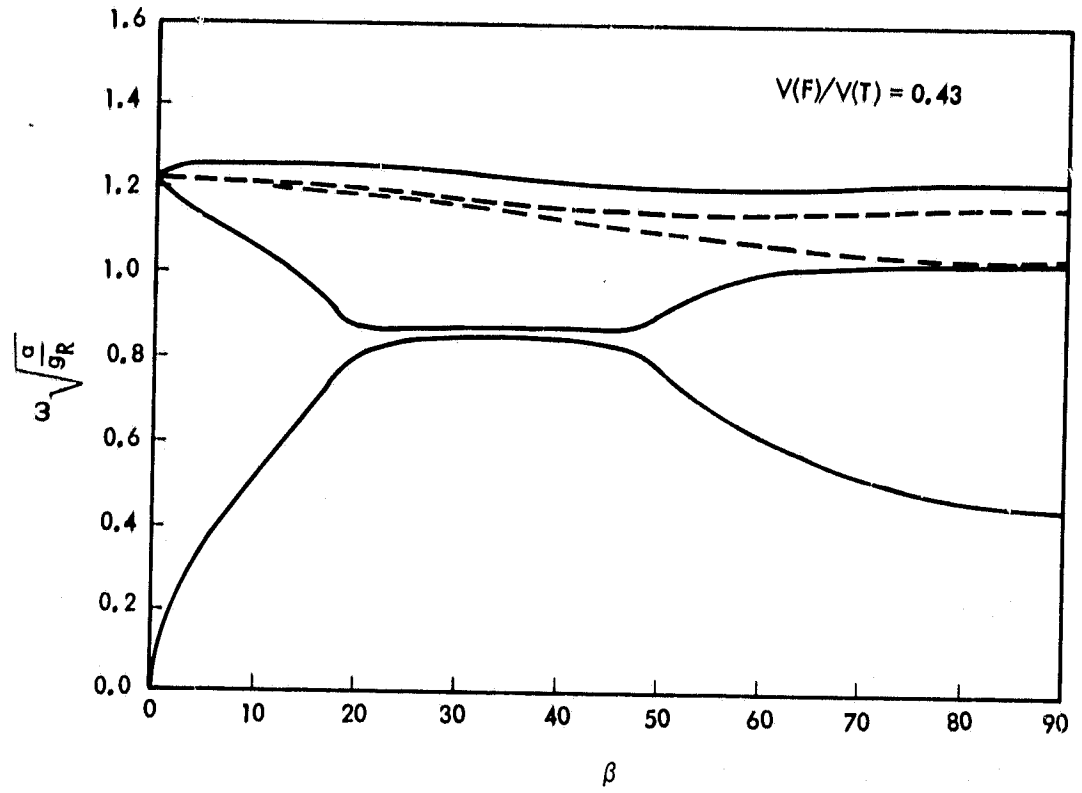

Figure 12a. Characteristic frequencies for $\tilde{V}$ = 0.43

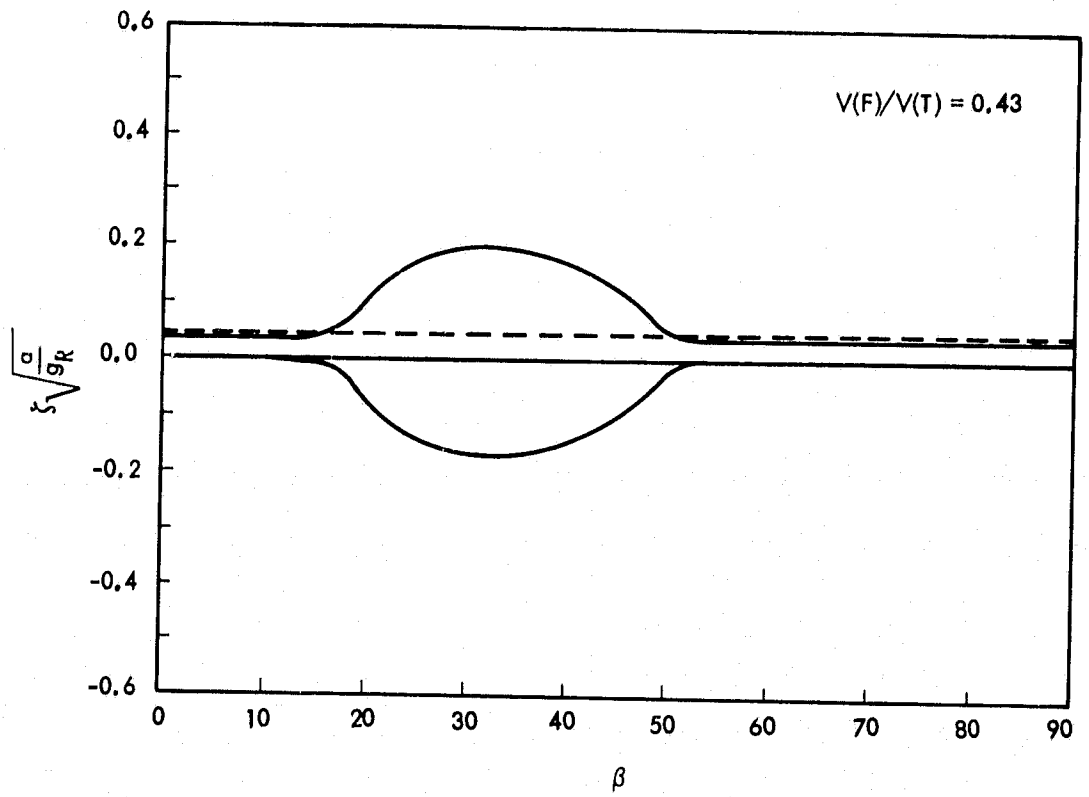

Figure 12b. Characteristic damping for $\tilde{V}$ = 0.43

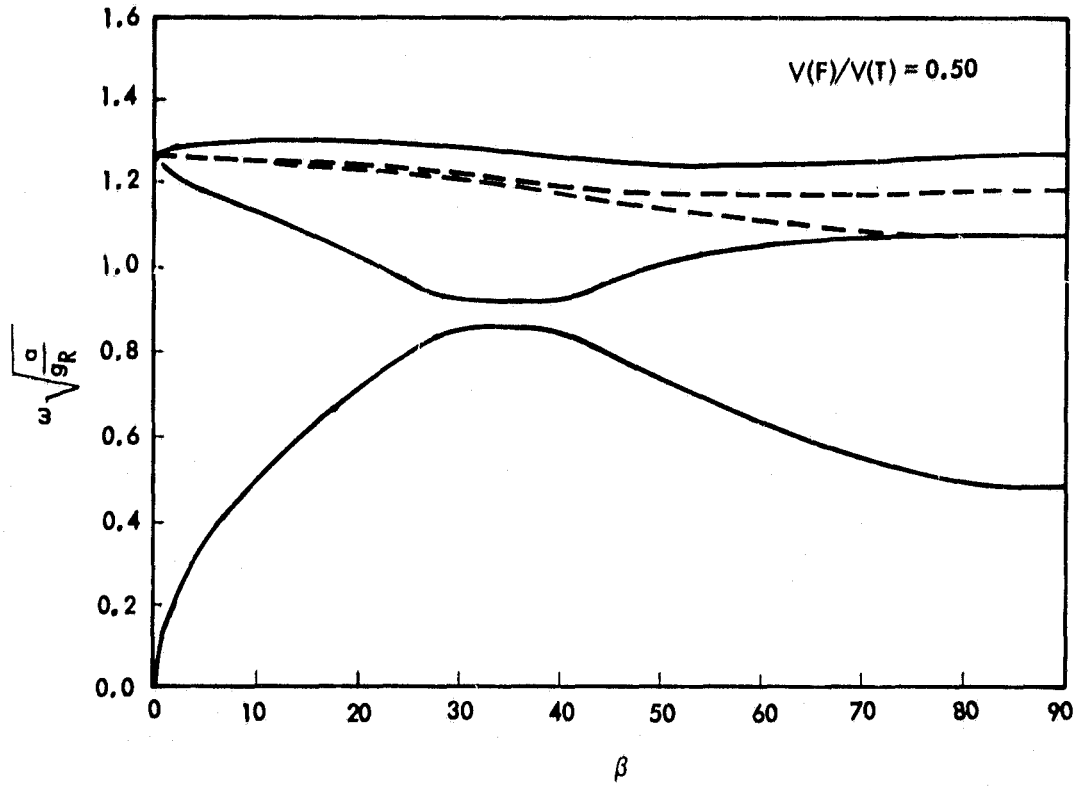

Figure 13a. Characteristic frequencies for $\tilde{V}$ = 0.50

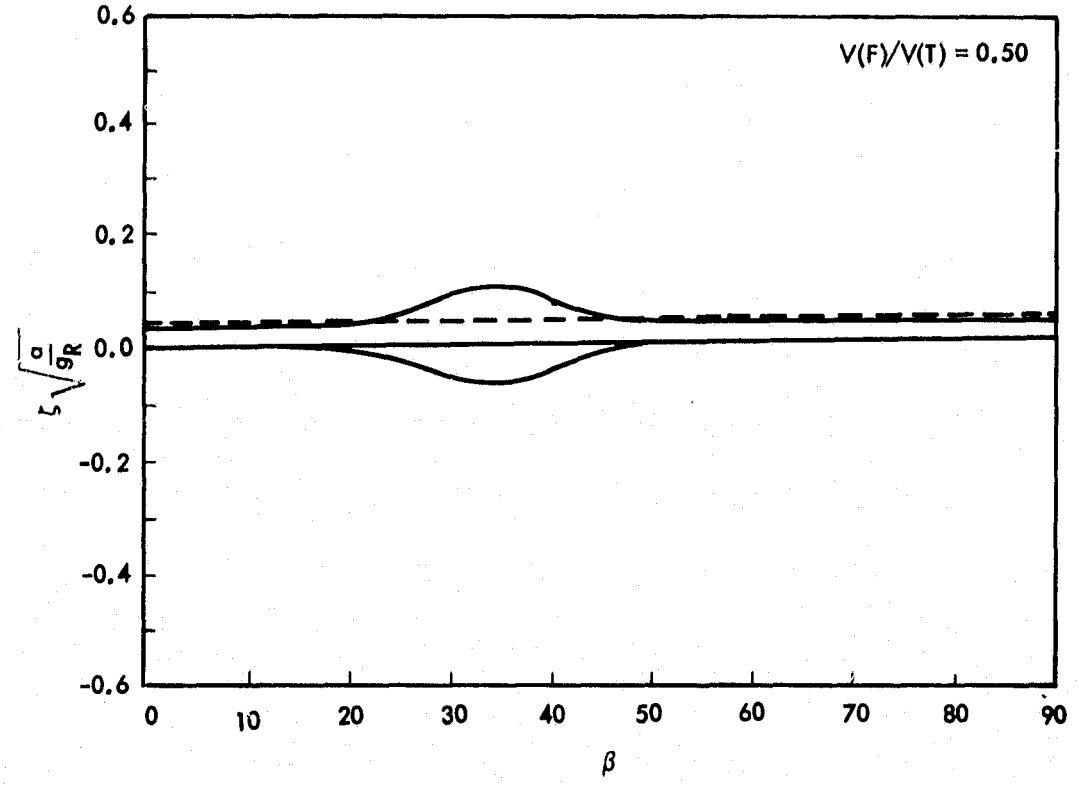

Figure 13b. Characteristic damping for $\tilde{V}$ = 0.50

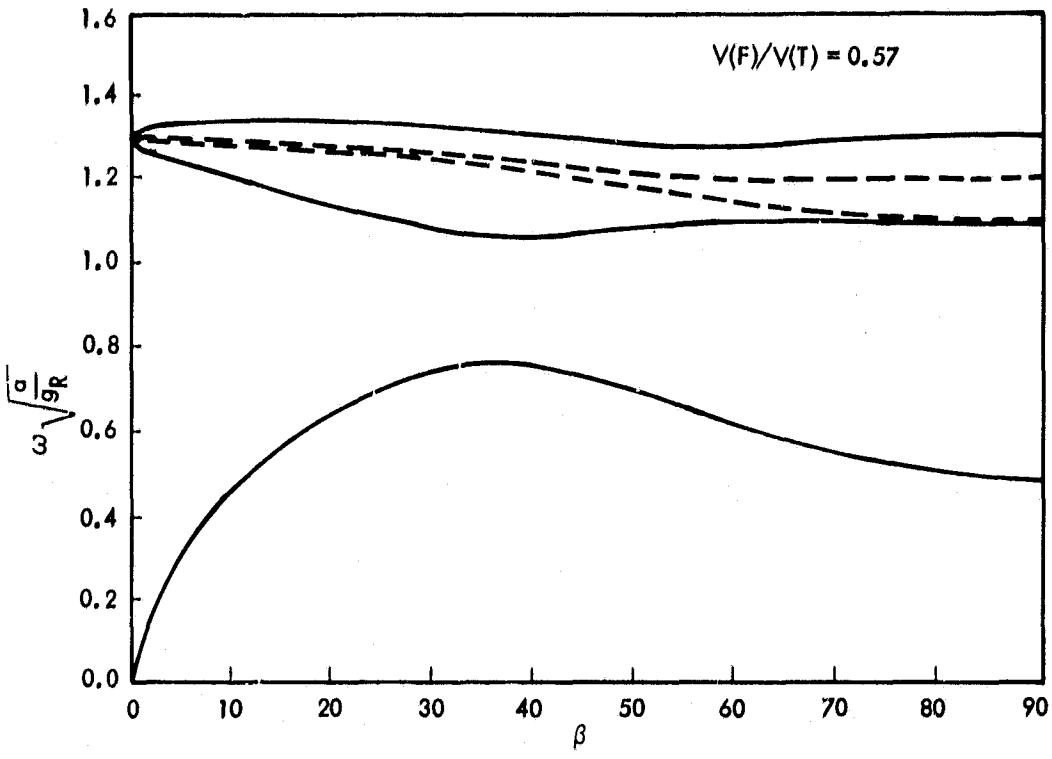

Figure 14a. Characteristic frequencies for $\tilde{V}$ = 0.57

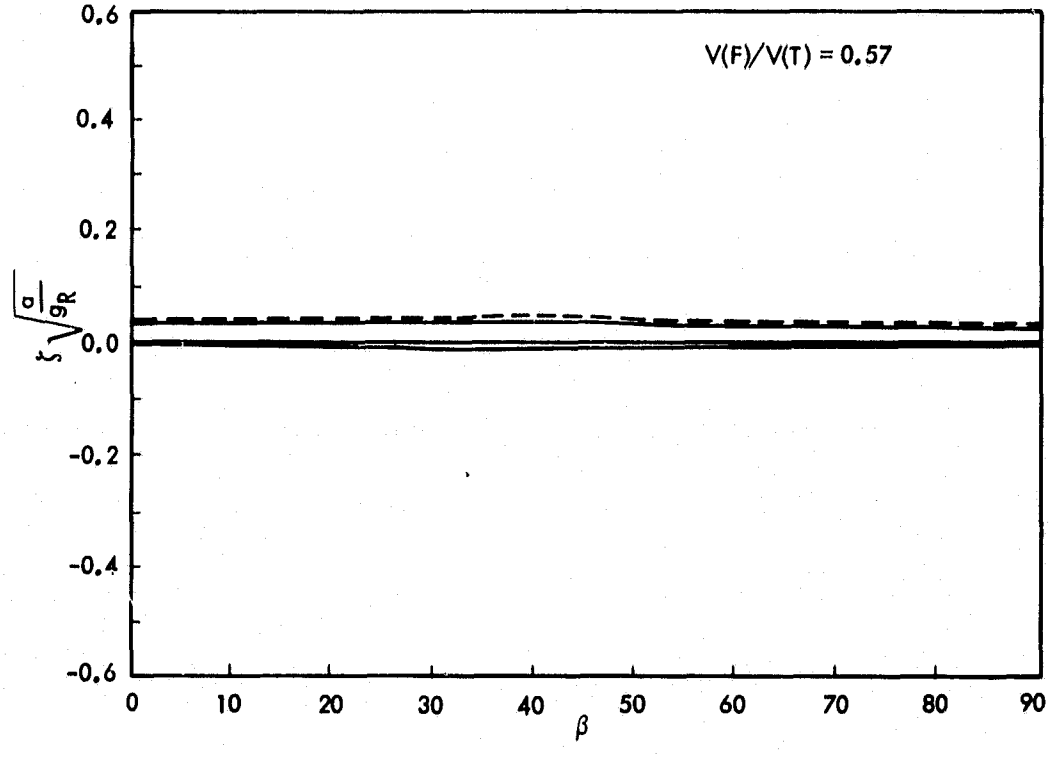

Figure 14b. Characteristic damping for $\tilde{V}$ = 0.57

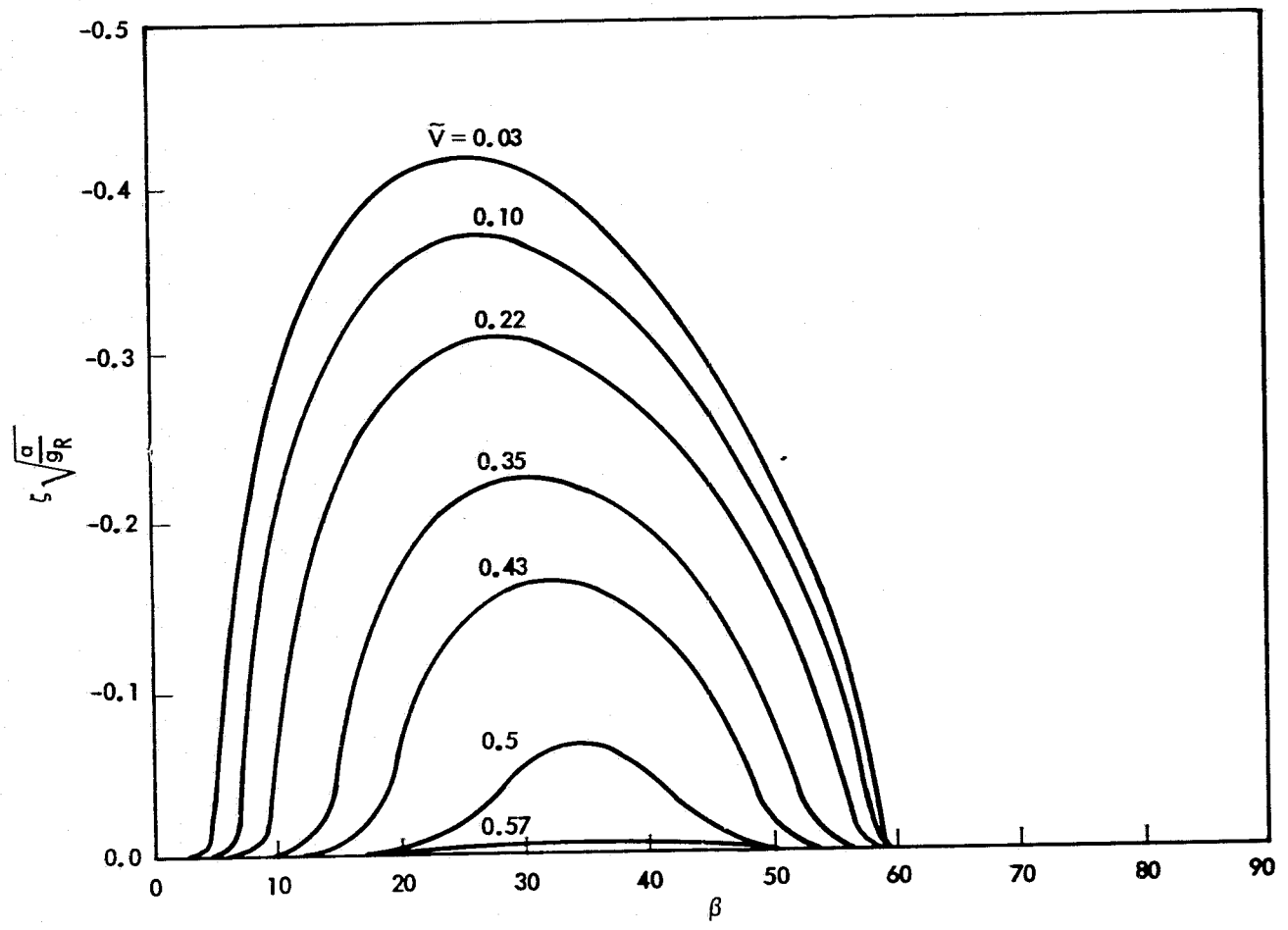

Figure 15. Variation of nondimensional negative damping with β